

Supporting Information

Ru(II)-Diphosphine/N,S-Mercapto Complexes and Their Anti-melanoma Properties

Nádija N. P. da Silva^a, Marcos V. Palmeira-Mello^a, Nathália O. Acésio^b, Carlos A. F. Moraes^a, João Honorato^c, Eduardo E. Castellano^c, Denise C. Tavares^b, Katia M. Oliveira^{d,*}, Alzir A. Batista^{a,*}

^a*Departament of Chemistry, Federal University of São Carlos – UFSCar, CEP 13565-905, São Carlos - SP, Brazil.*

^b*University of Franca - UNIFRAN, Avenida Dr. Armando Salles Oliveira, CP 201, Parque Universitário, CEP 14404-600, Franca, SP, Brazil.*

^c*Physics Institute of São Carlos, University of São Paulo – USP, CEP 13560-970, São Carlos, SP, Brazil.*

^d*Institute of Chemistry, University of Brasília - UnB – CEP 70910-900, Brasília - DF, Brazil.*

* Corresponding authors: katia.oliveira@unb.br (Katia M. Oliveira); daab@ufscar.br (Alzir A. Batista)

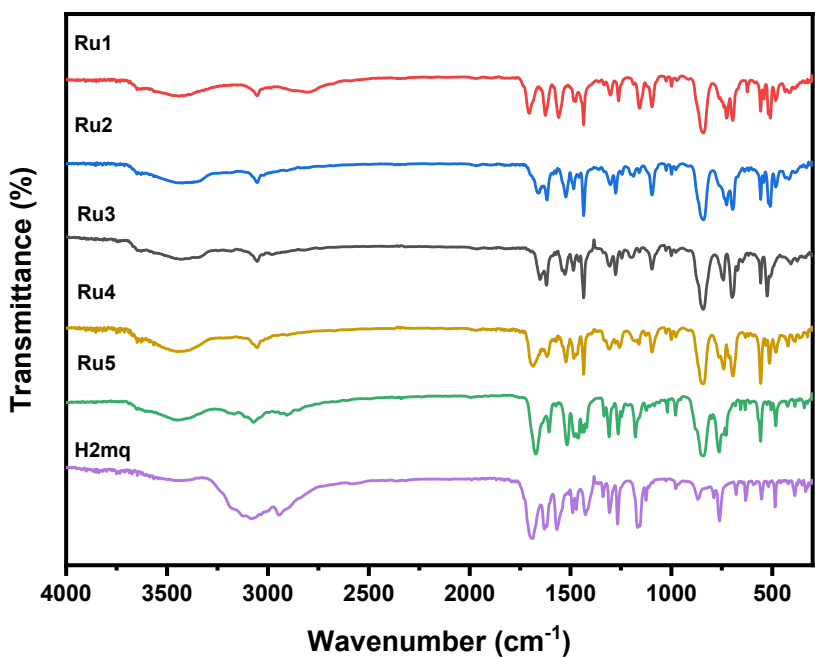


Figure S1. FTIR spectra of the free **H2mq** ligand and **Ru1-Ru5** complexes, in KBr pellets.

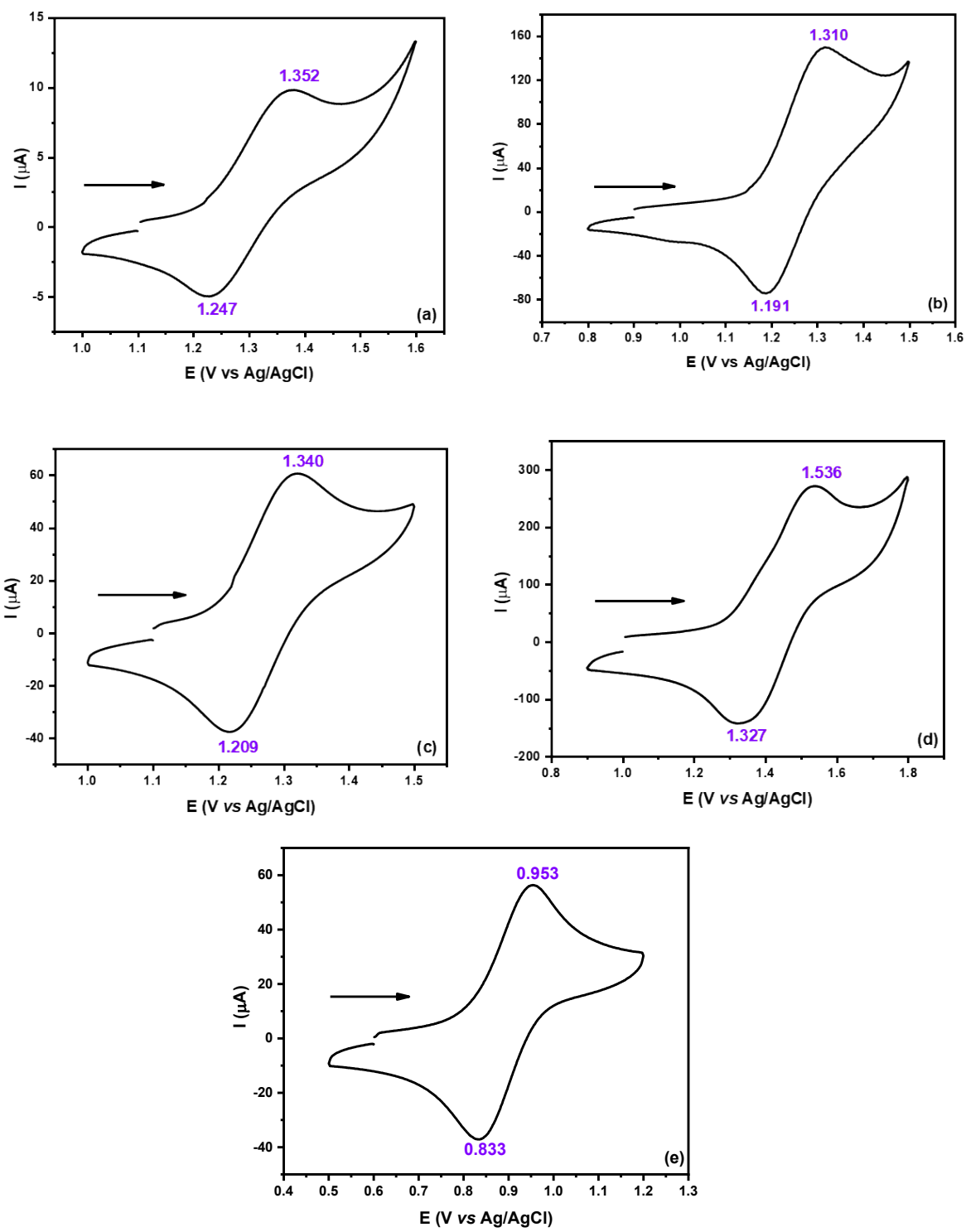


Figure S2. (A-E) Cyclic voltammogram (Electrolyte: 0.1 M PTBA in CH_2Cl_2 ; Electrodes: Ag/AgCl , as a reference and Pt disc as work and auxiliary, 100 mVs^{-1}) of **Ru1-Ru5** complexes.

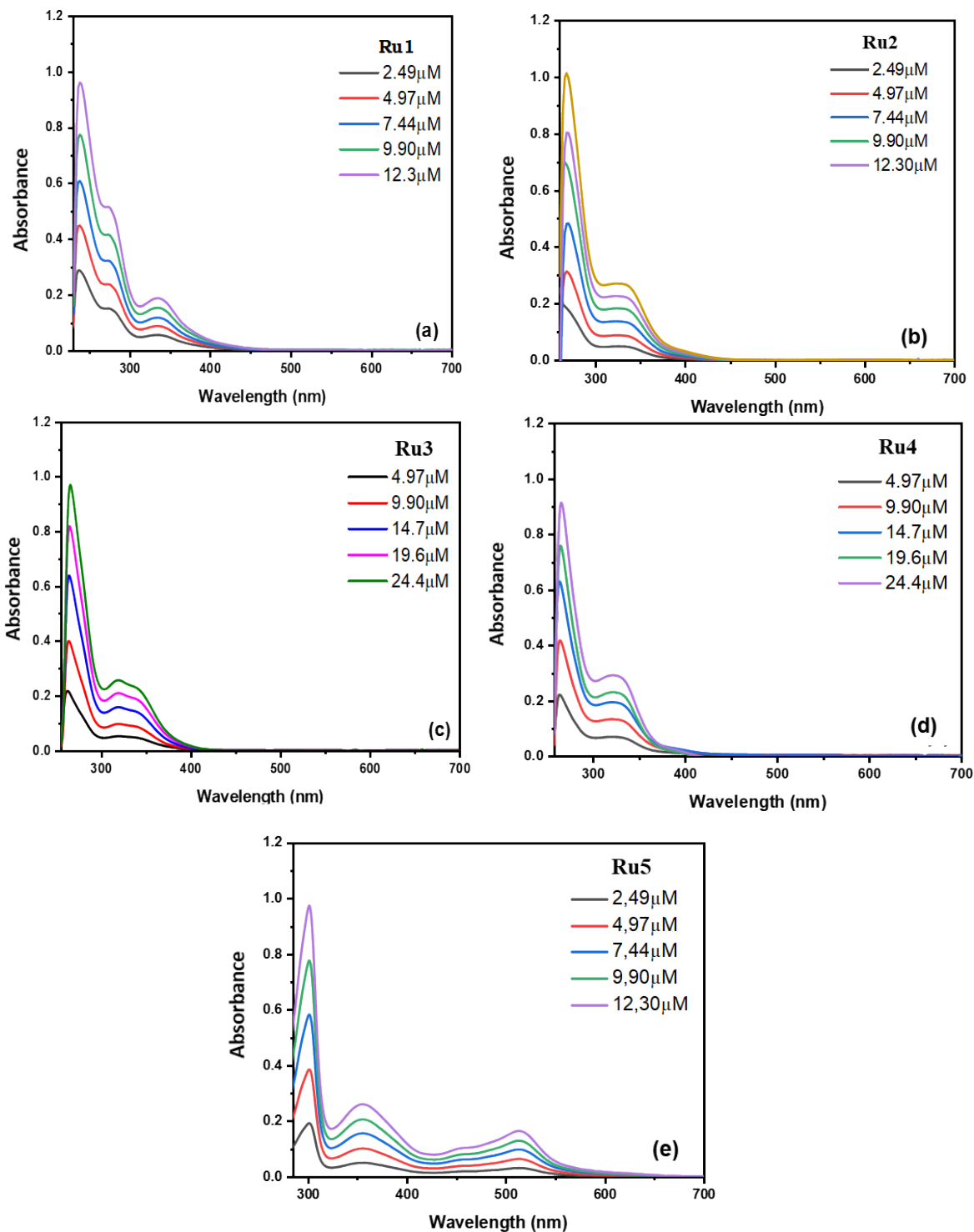


Figure S3. (A) UV-vis spectra of the **Ru1** complex in CH_2Cl_2 . (B-E) UV-vis spectra of the **Ru2- Ru5** complex in DMSO.

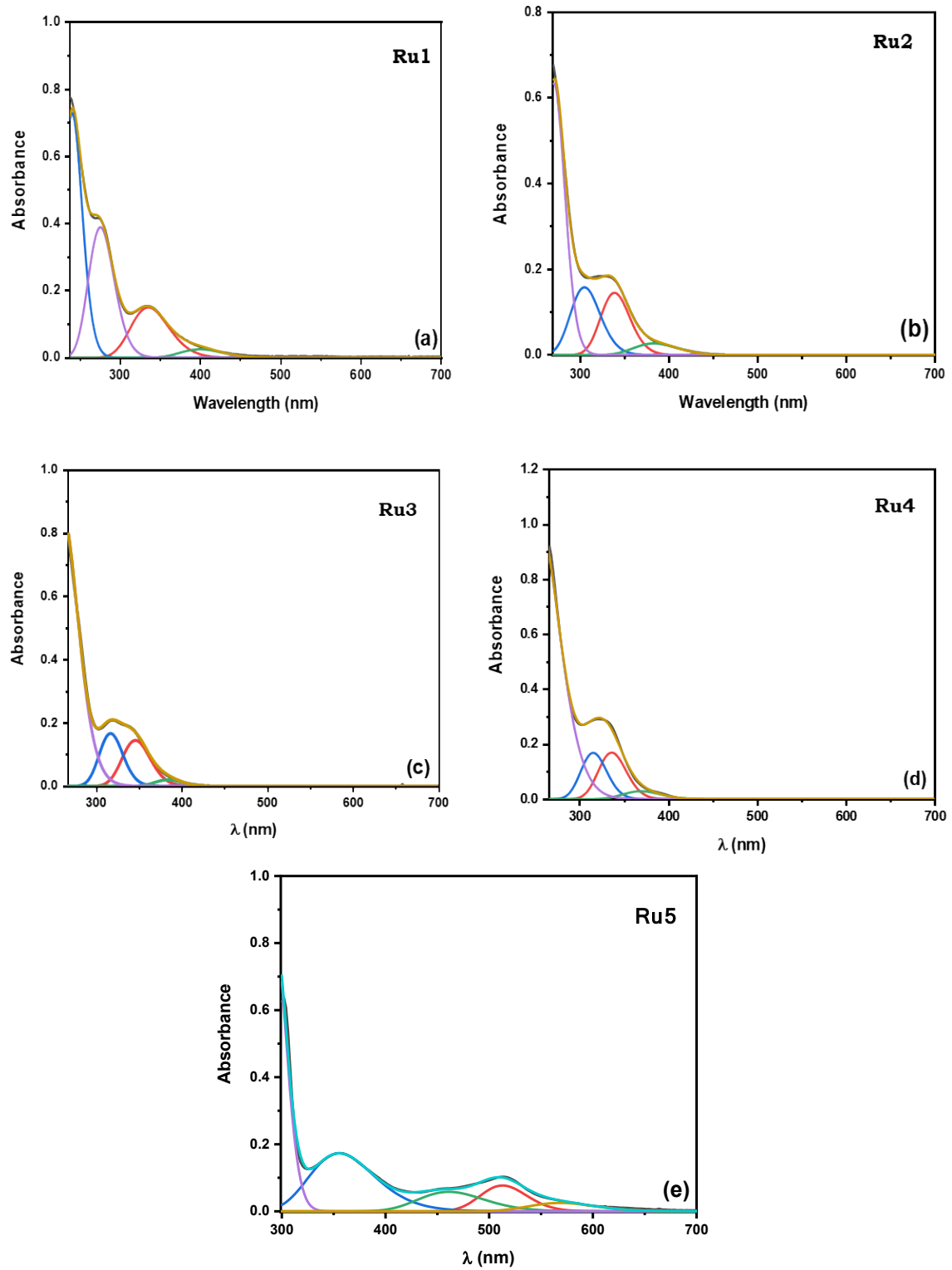


Figure S4. (A-E) Deconvolution of the electronic spectra of **Ru1-Ru5** complexes.

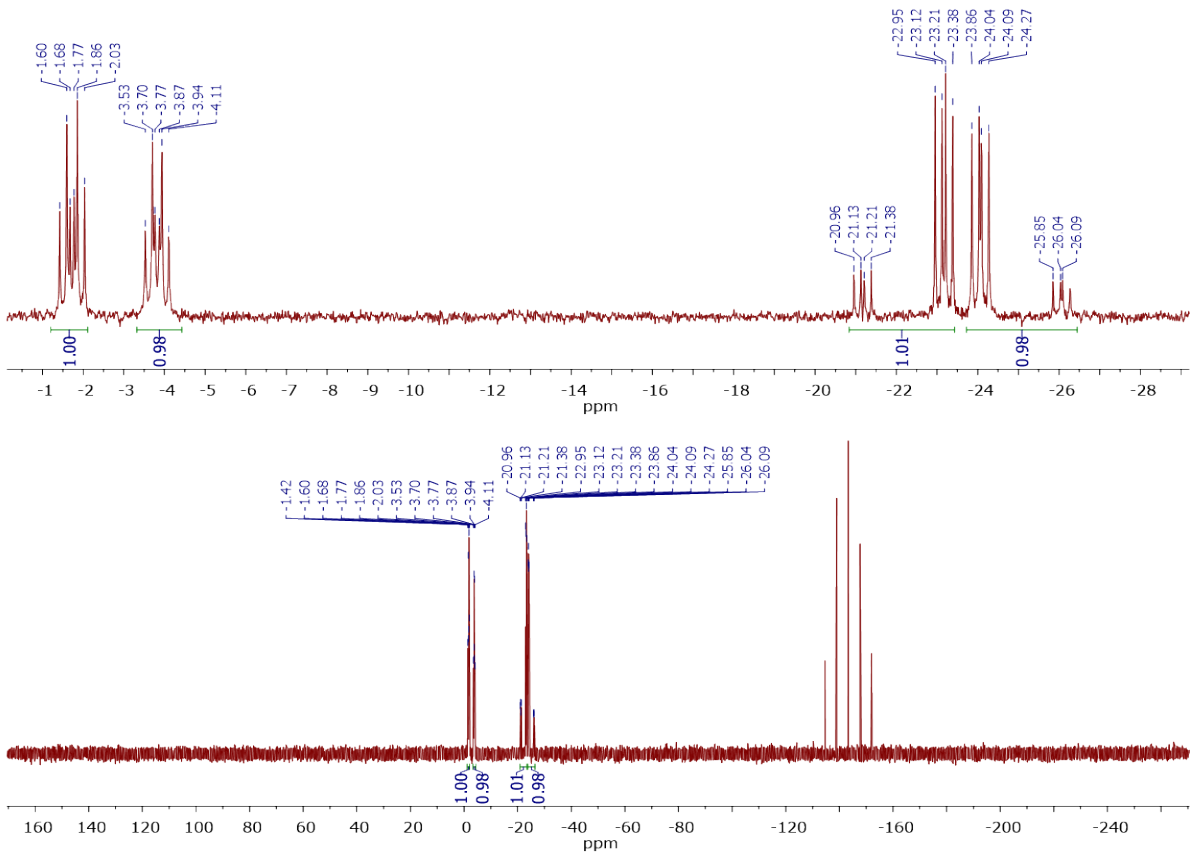


Figure S5. $^{31}\text{P}\{\text{H}\}$ NMR spectrum of the Ru1 complex in acetone/D₂O.

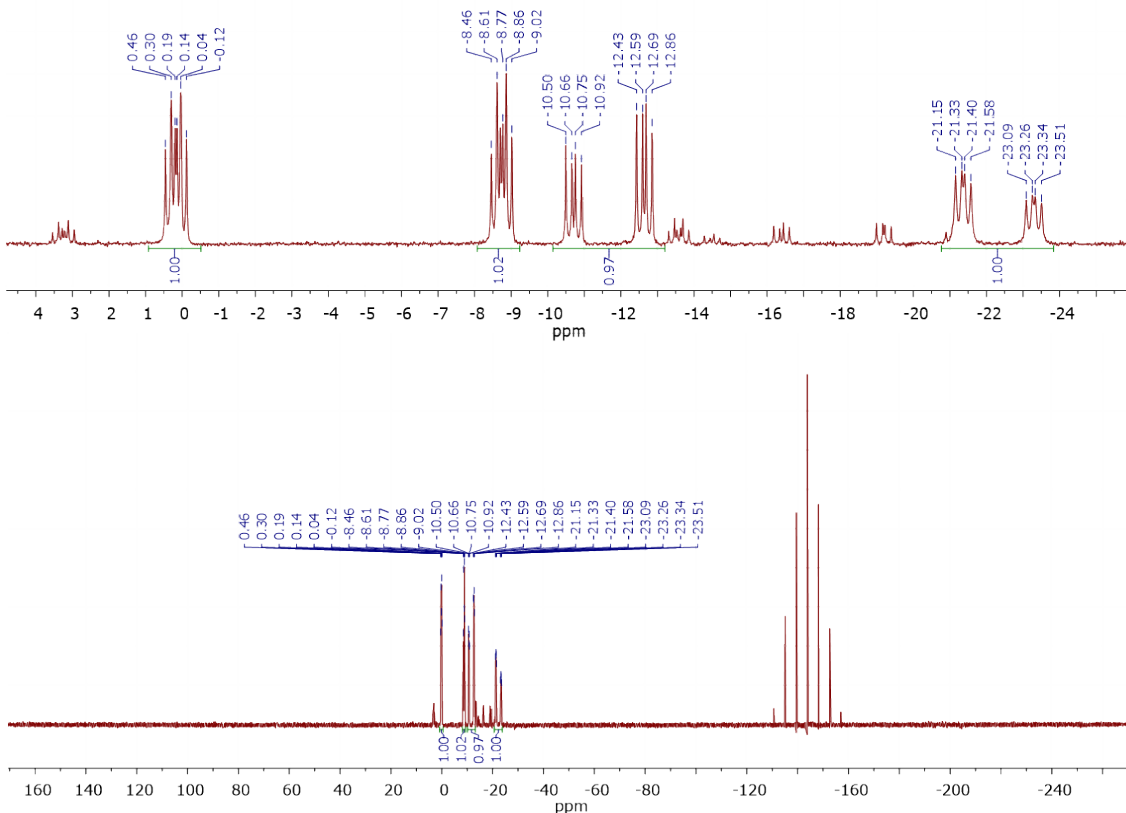


Figure S6. $^{31}\text{P}\{^1\text{H}\}$ NMR spectrum of the Ru2 complex in DMSO/D₂O.

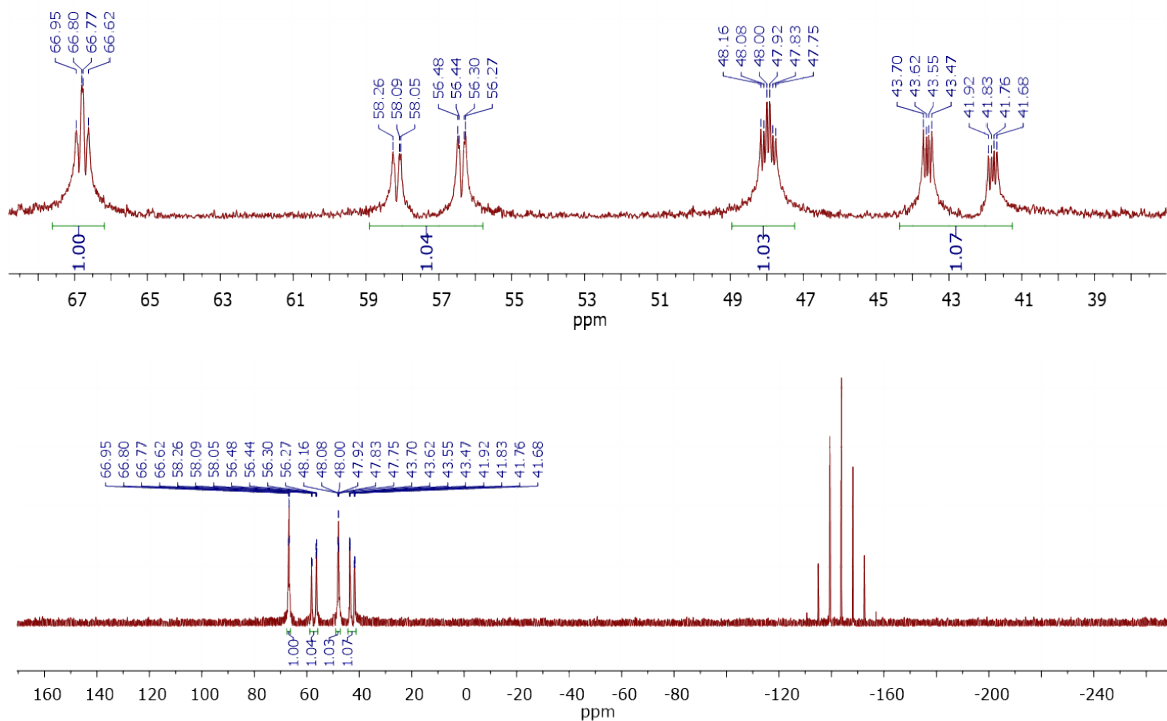


Figure S7. $^{31}\text{P}\{^1\text{H}\}$ NMR spectrum of the Ru3 complex in DMSO/D₂O.

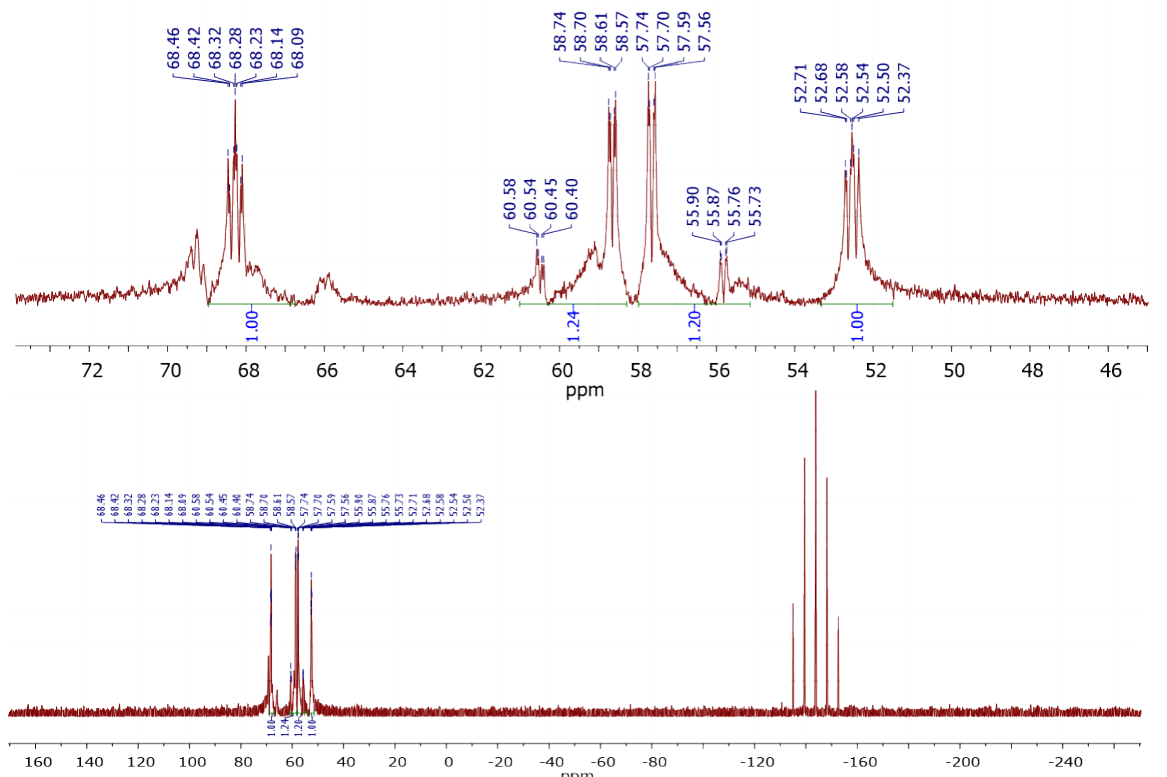


Figure S8. $^{31}\text{P}\{^1\text{H}\}$ NMR spectrum of the Ru4 complex in DMSO/D₂O.

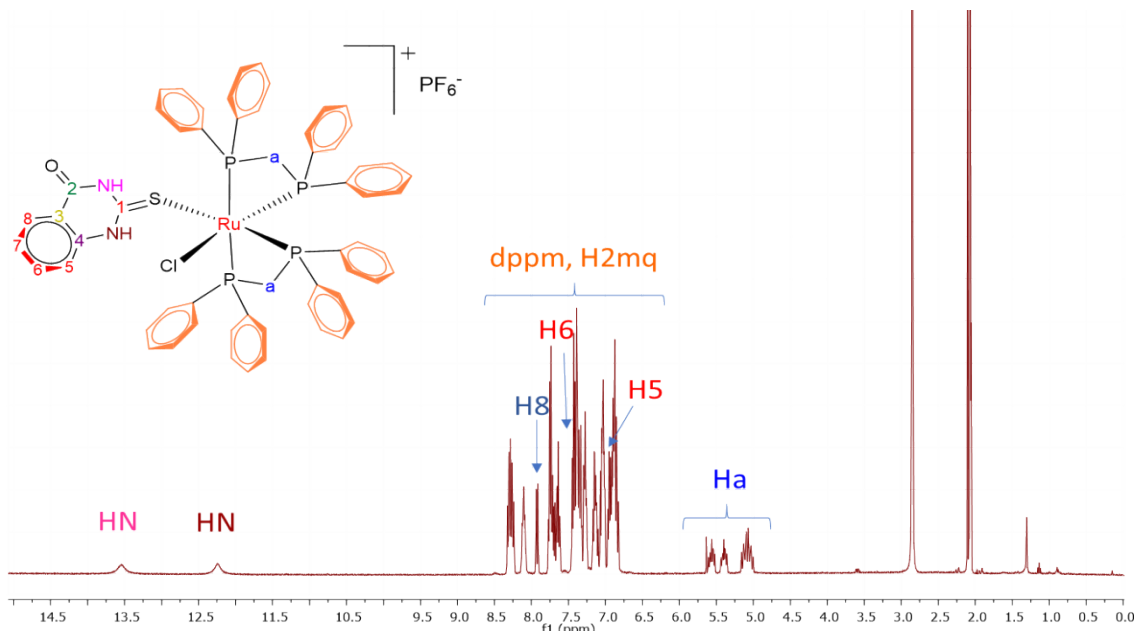


Figure S9. ^1H NMR spectrum of the Ru1 complex in acetone- d_6 .

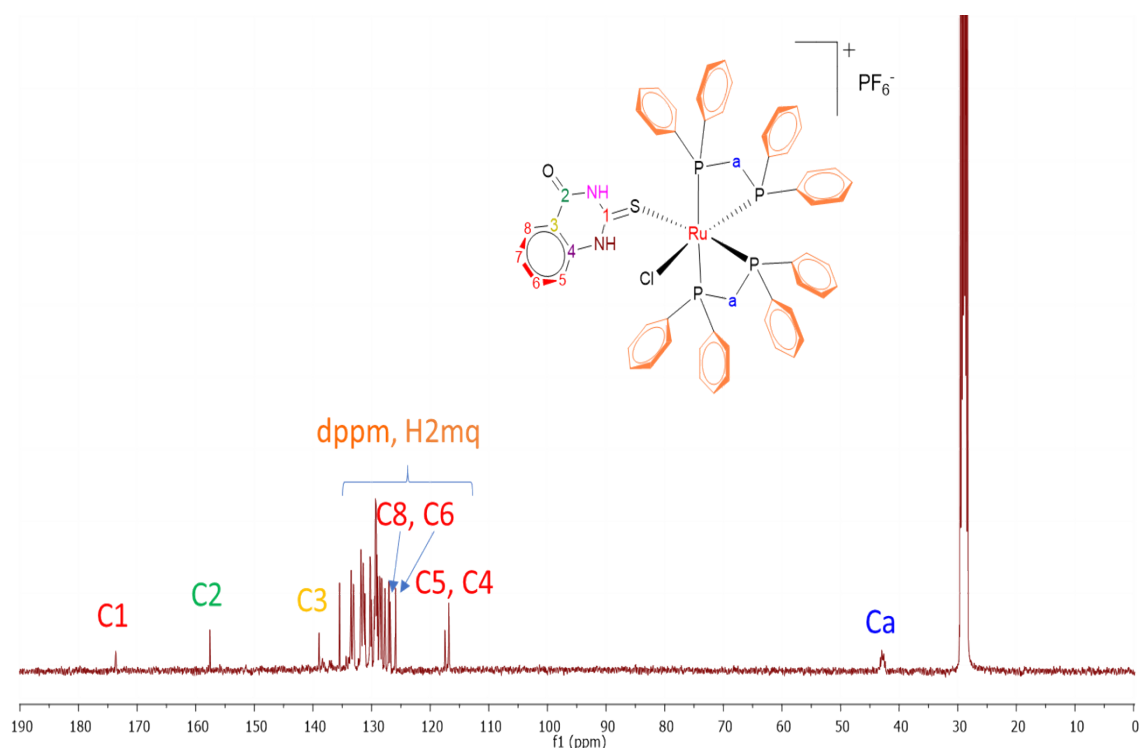


Figure S10. $^{13}\text{C}\{^1\text{H}\}$ NMR spectrum of the Ru1 complex in acetone- d_6 .

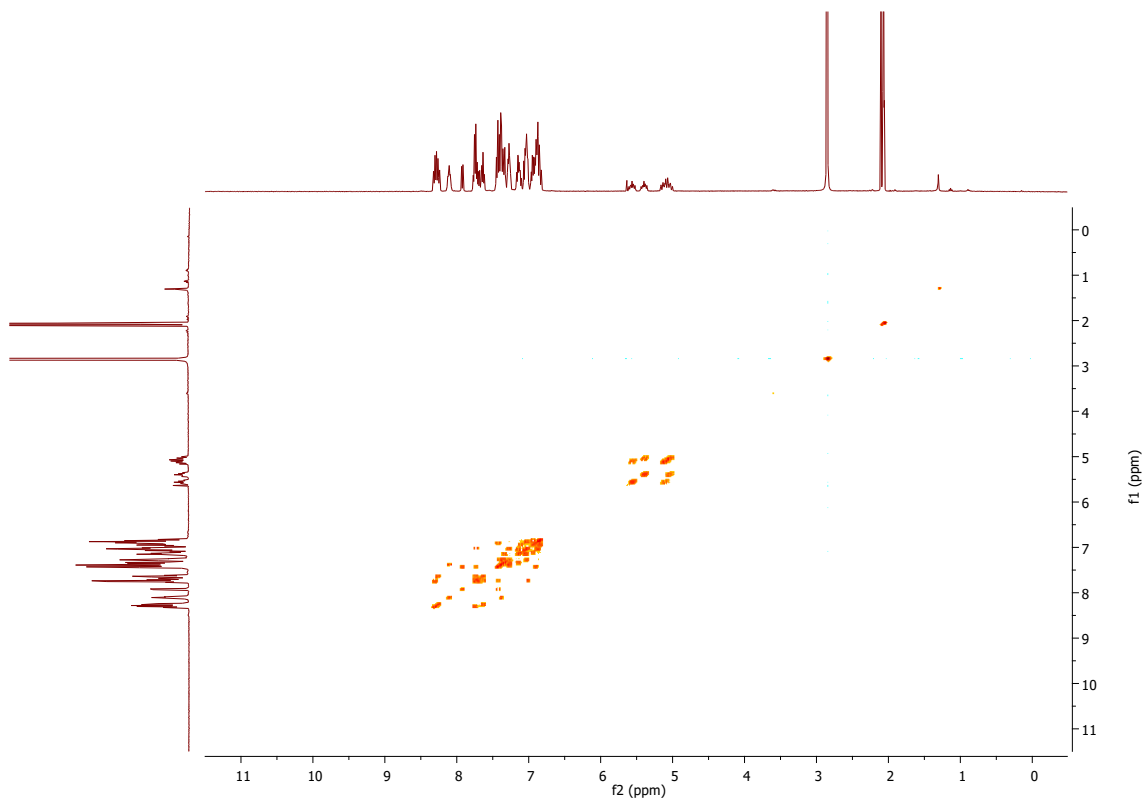


Figure S11. Contour map of the ^1H - ^1H COSY correlation obtained for the Ru1 complex (acetone- d_6).

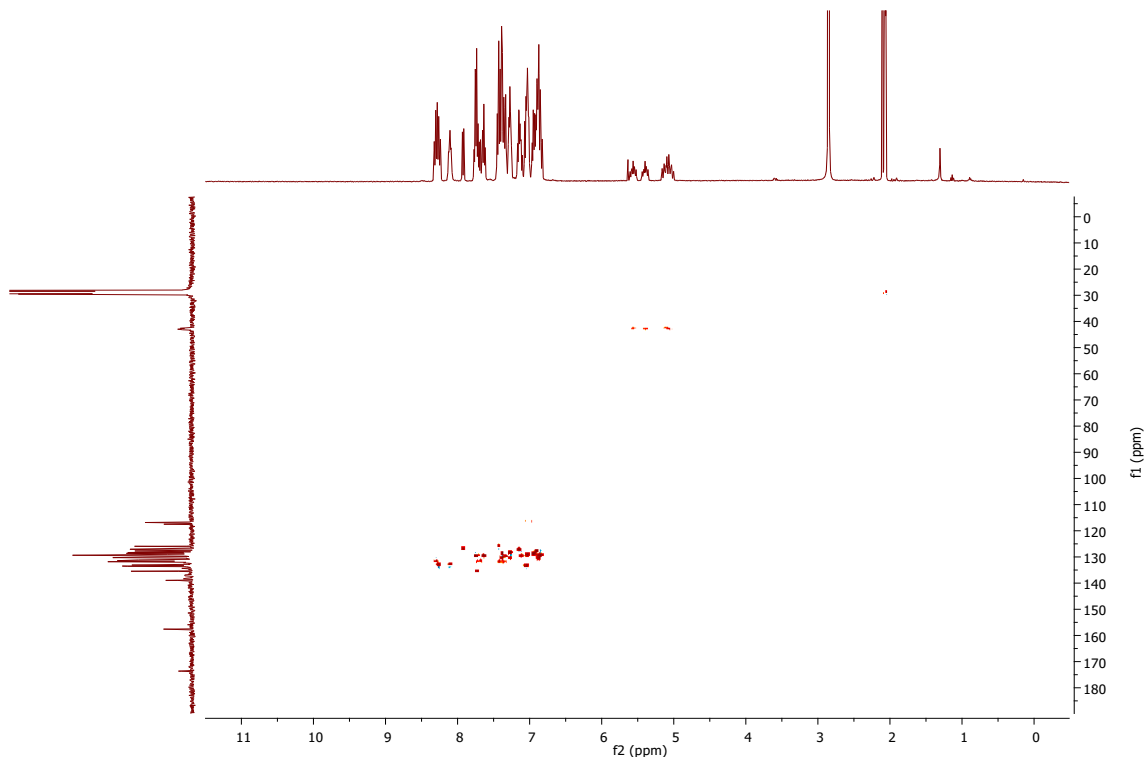


Figure S12. Contour map of the ^1H - ^{13}C HSCQ correlation obtained for the Ru1 complex (acetone- d_6).

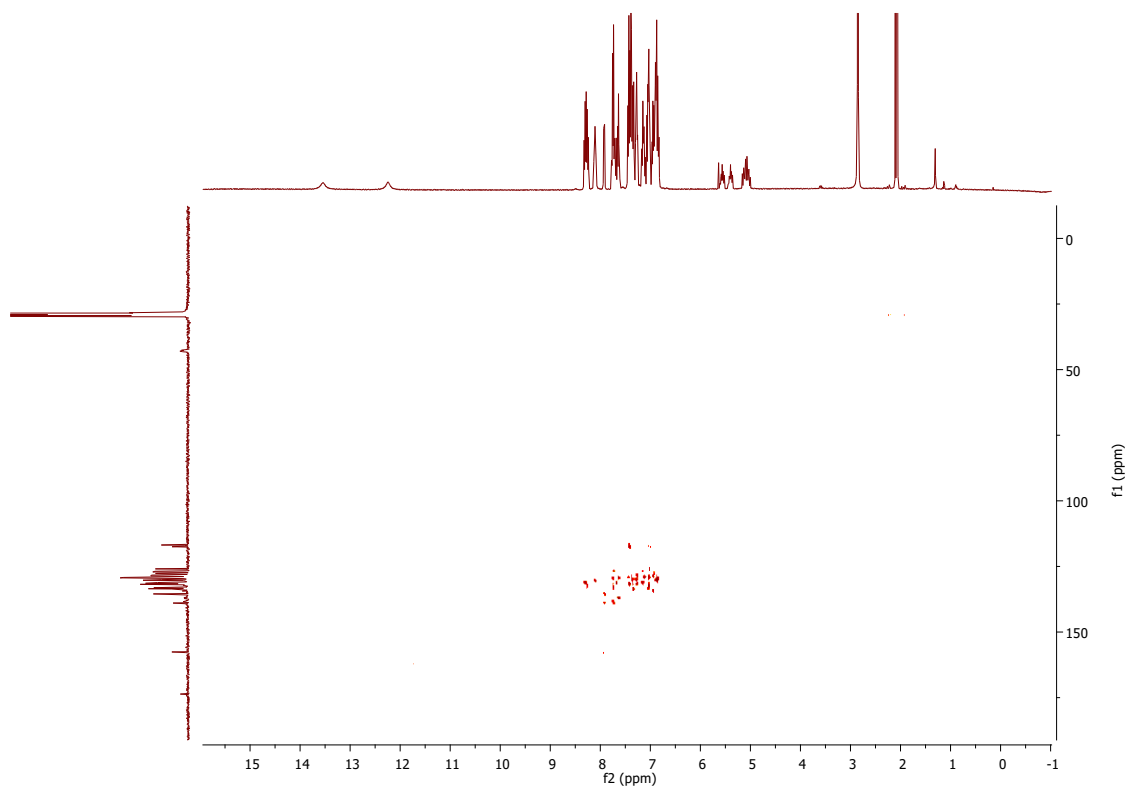


Figure S13. Contour map of the ¹H-¹³C HMBC correlation obtained for the Ru1 complex (acetone-d₆).

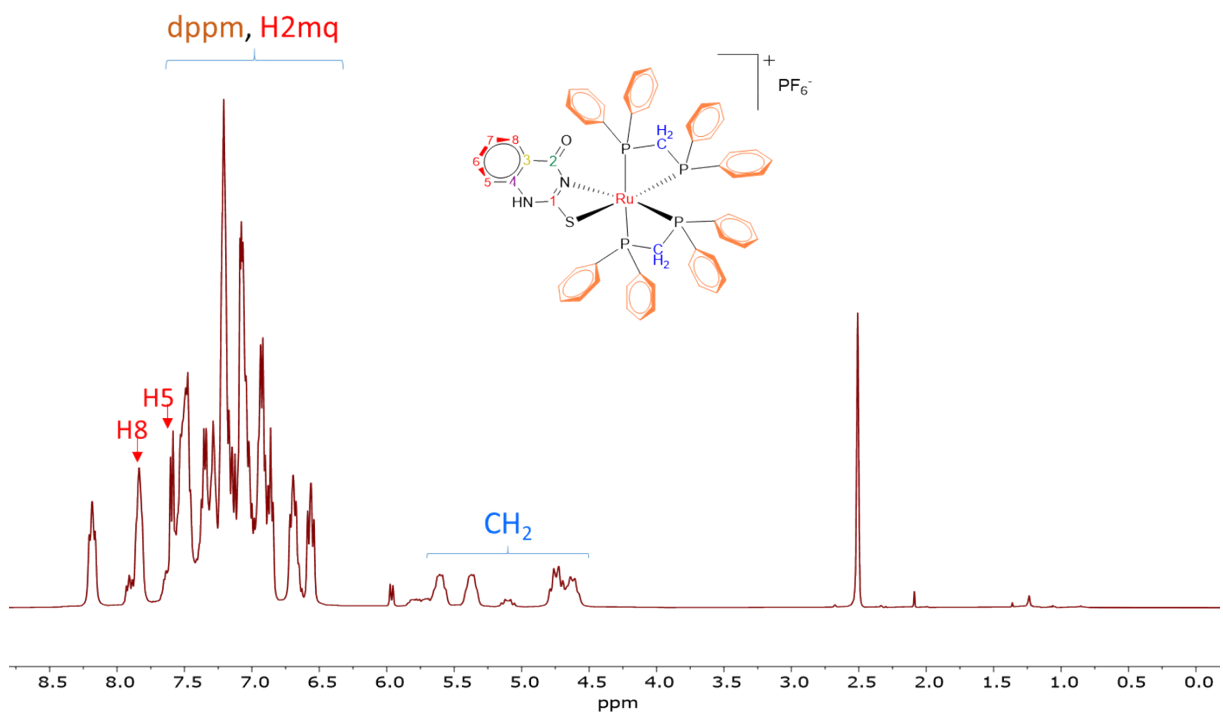


Figure S14. ¹H NMR spectrum of the Ru2 complex in DMSO-d₆.

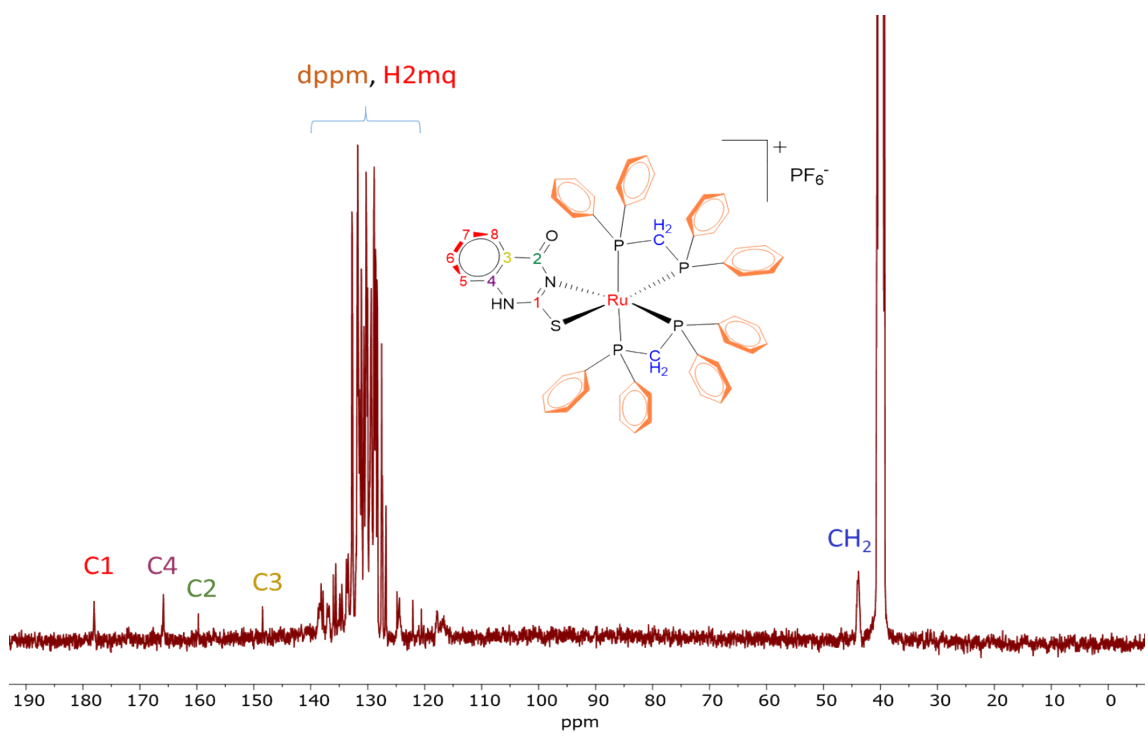


Figure S15. ^{13}C { ^1H } NMR spectrum of the **Ru2** complex in DMSO-d_6 .

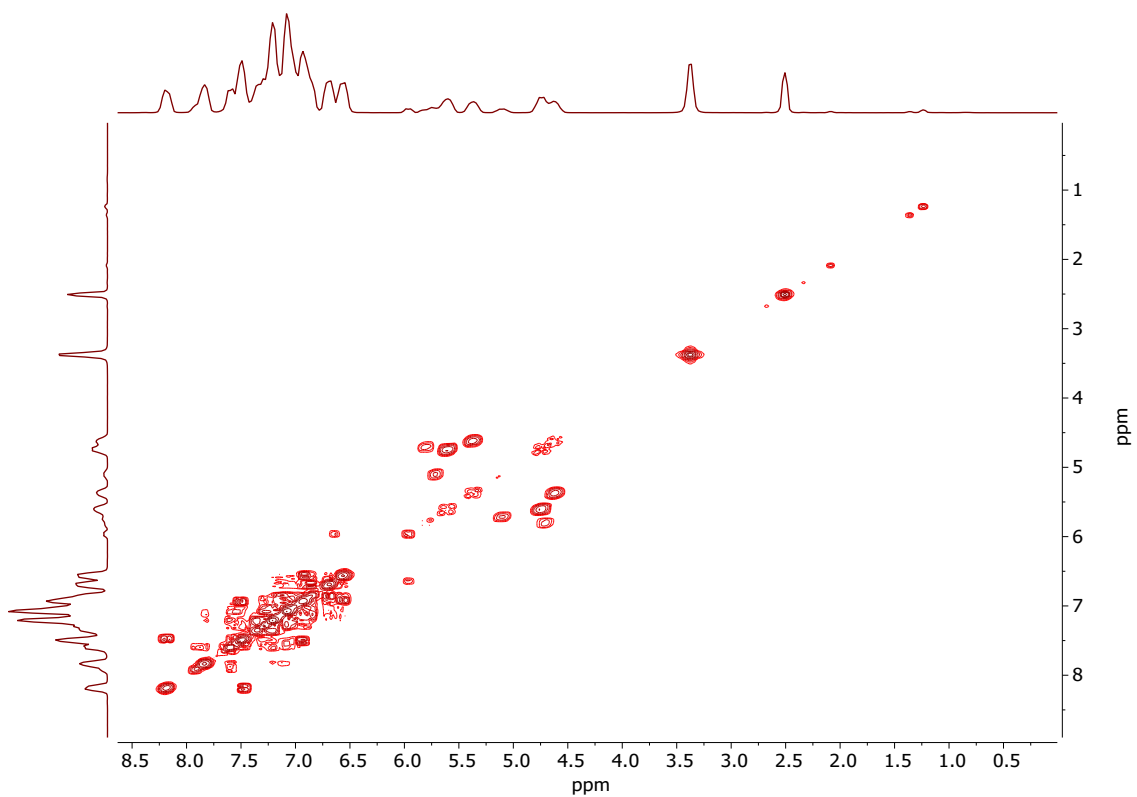


Figure S16. Contour map of the ^1H - ^1H COSY correlation obtained for the **Ru2** complex (DMSO-d_6).

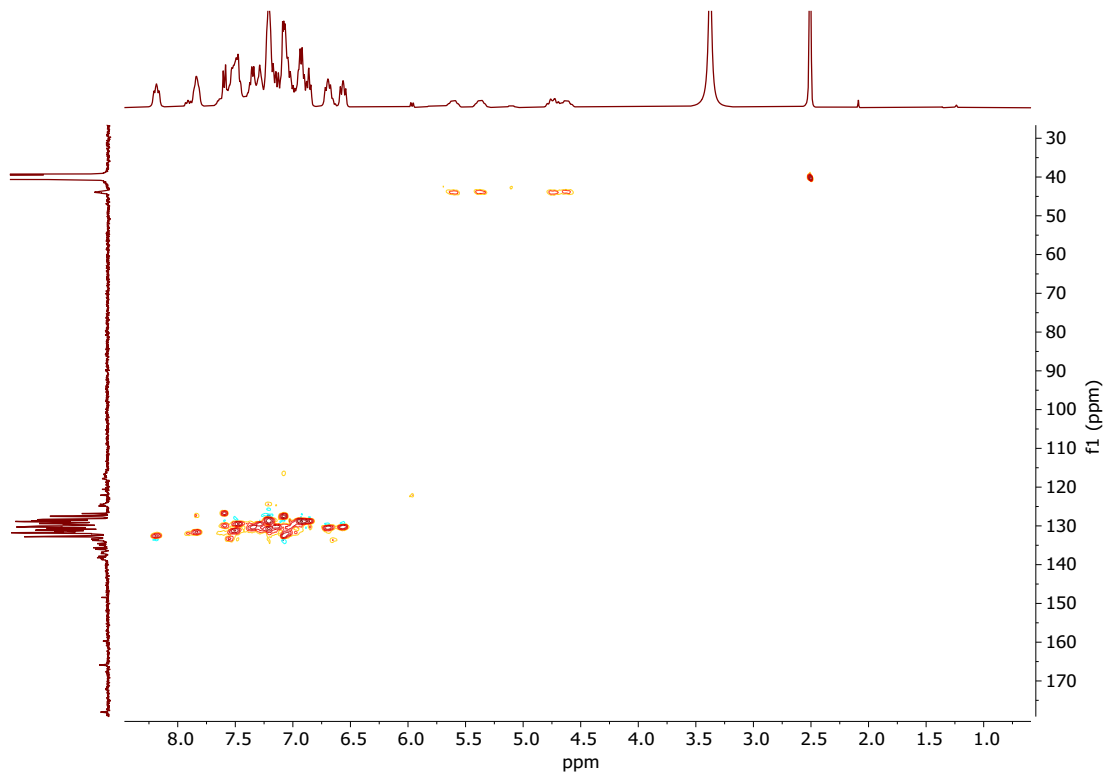


Figure S17. Contour map of the ^1H - ^{13}C HSQC correlation obtained for the **Ru2** complex (DMSO- d_6).

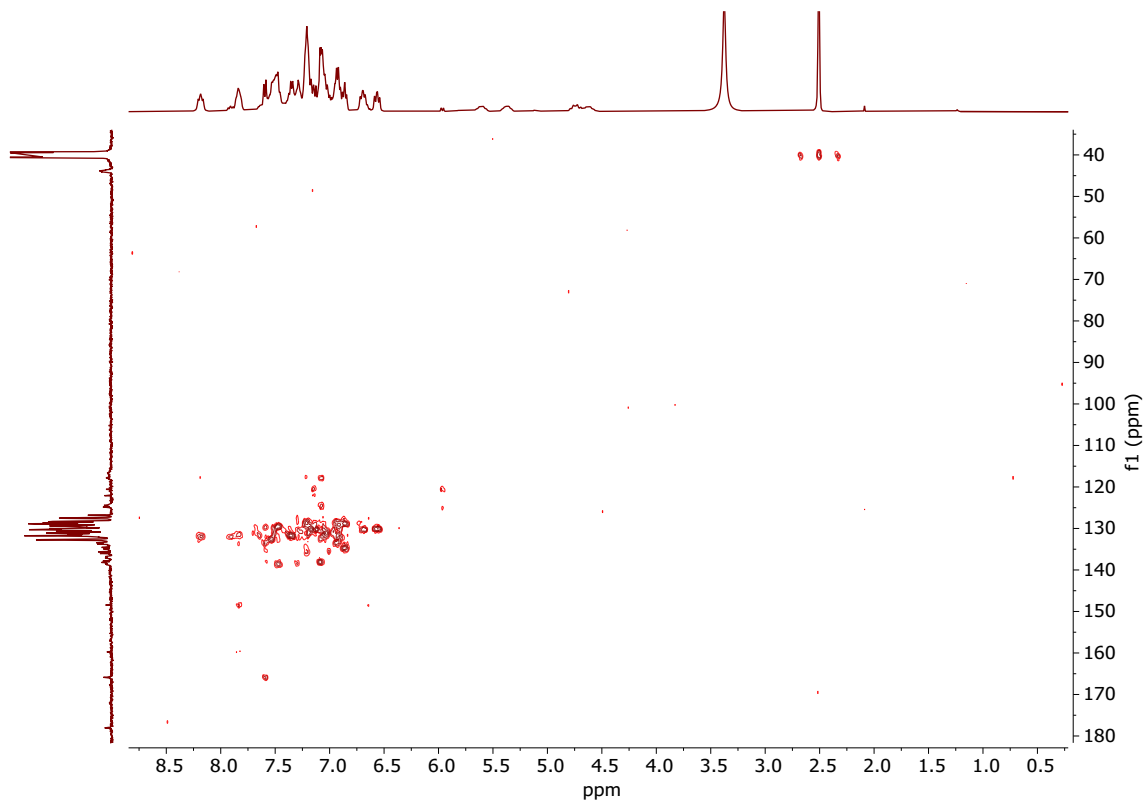


Figure S18. Contour map of the ^1H - ^{13}C HMBC correlation obtained for the **Ru2** complex (DMSO- d_6).

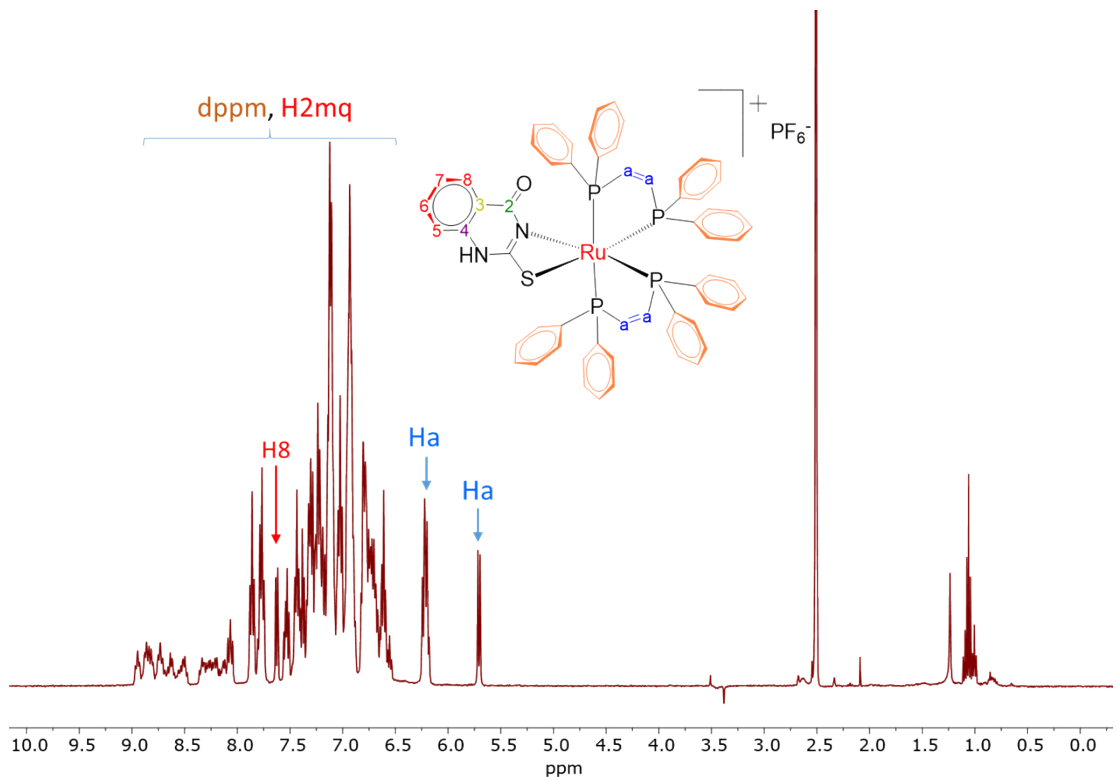


Figure S19. ^1H NMR spectrum of the Ru4 complex in DMSO-d_6 .

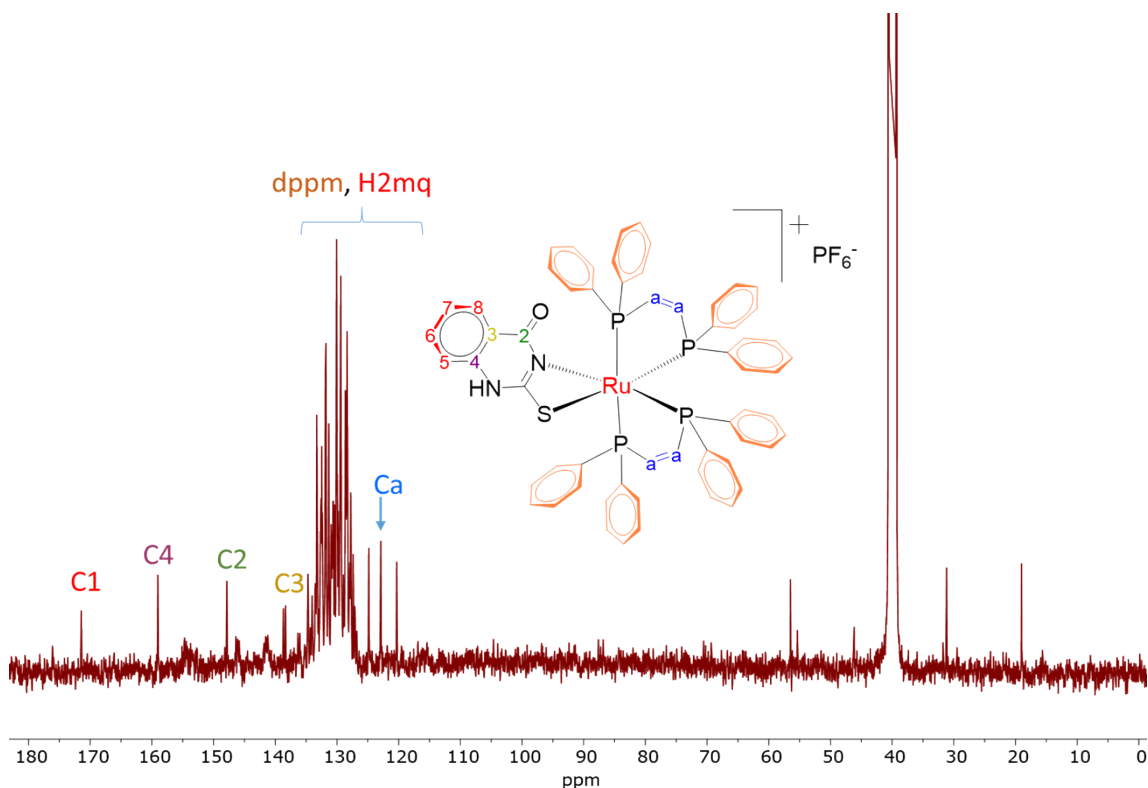


Figure S20. $^{13}\text{C}\{\text{H}\}$ NMR spectrum of the Ru4 complex in DMSO-d_6 .

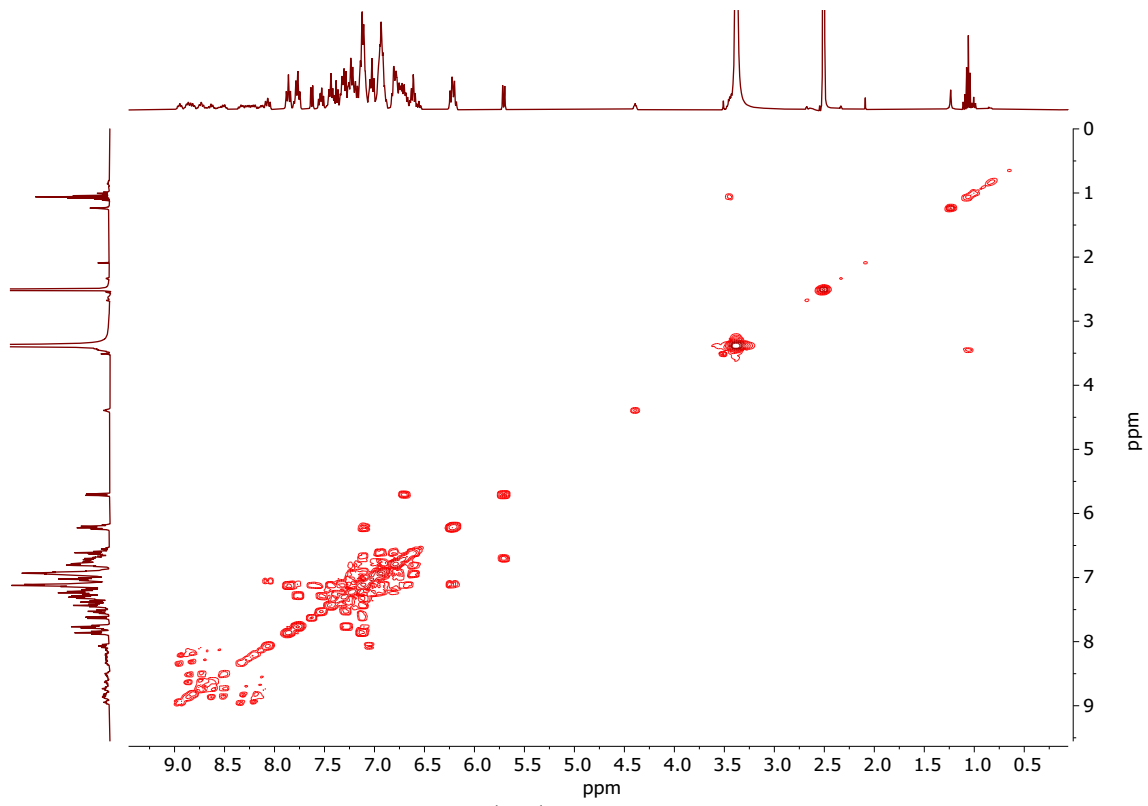


Figure S21. Contour map of the ¹H-¹H COSY correlation obtained for the **Ru4** complex (DMSO-d₆).

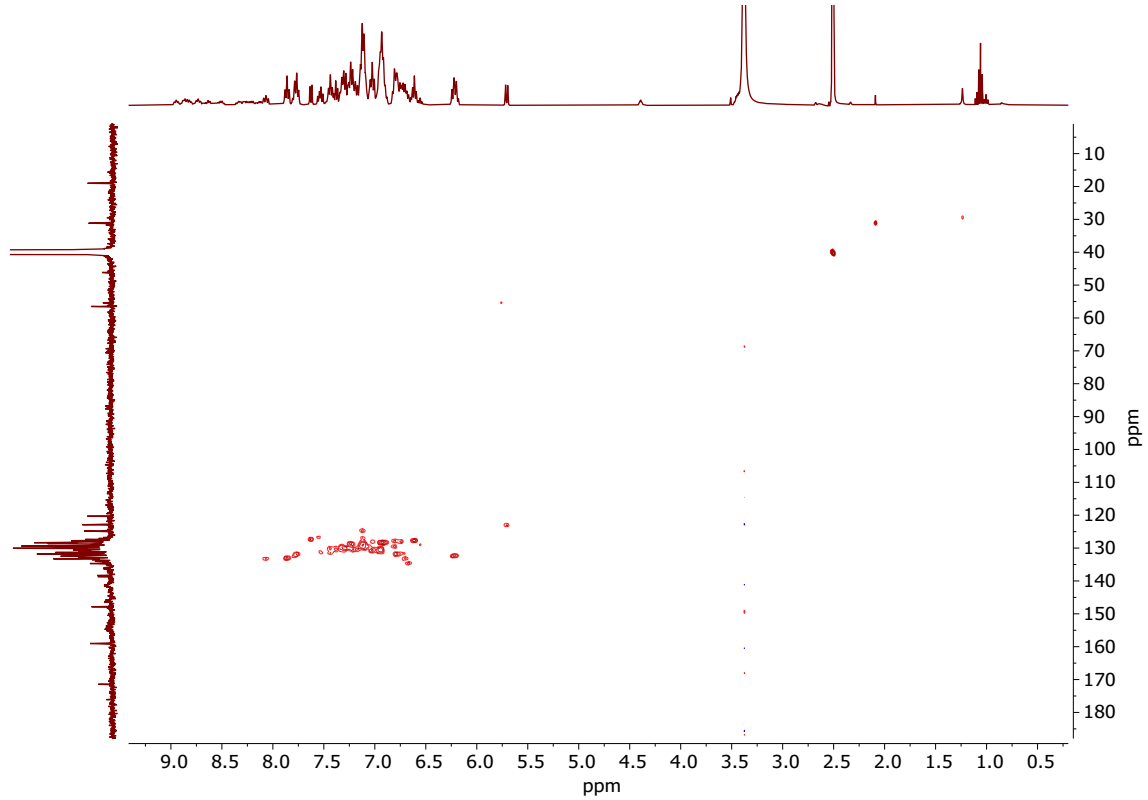


Figure S22. Contour map of the ^1H - ^{13}C HSQC correlation obtained for the **Ru4** complex (DMSO- d_6).

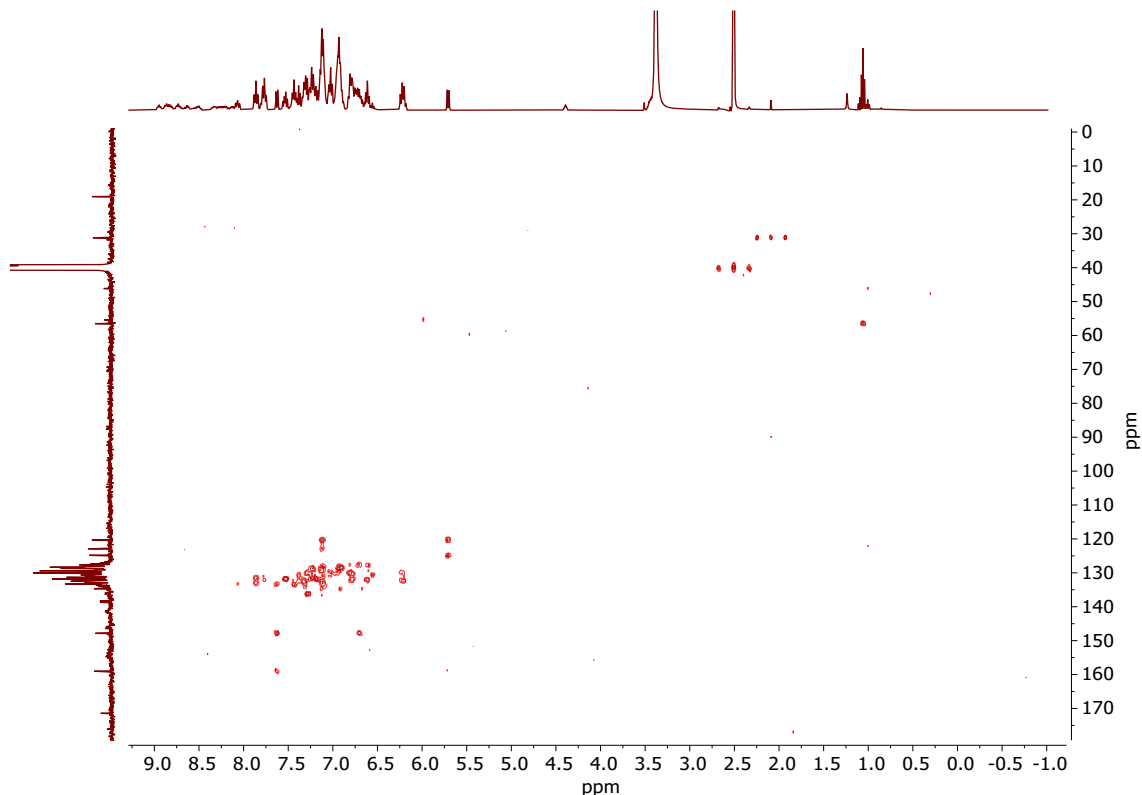


Figure S23. Contour map of the ^1H - ^{13}C HMBC correlation obtained for the **Ru4** complex (DMSO- d_6).

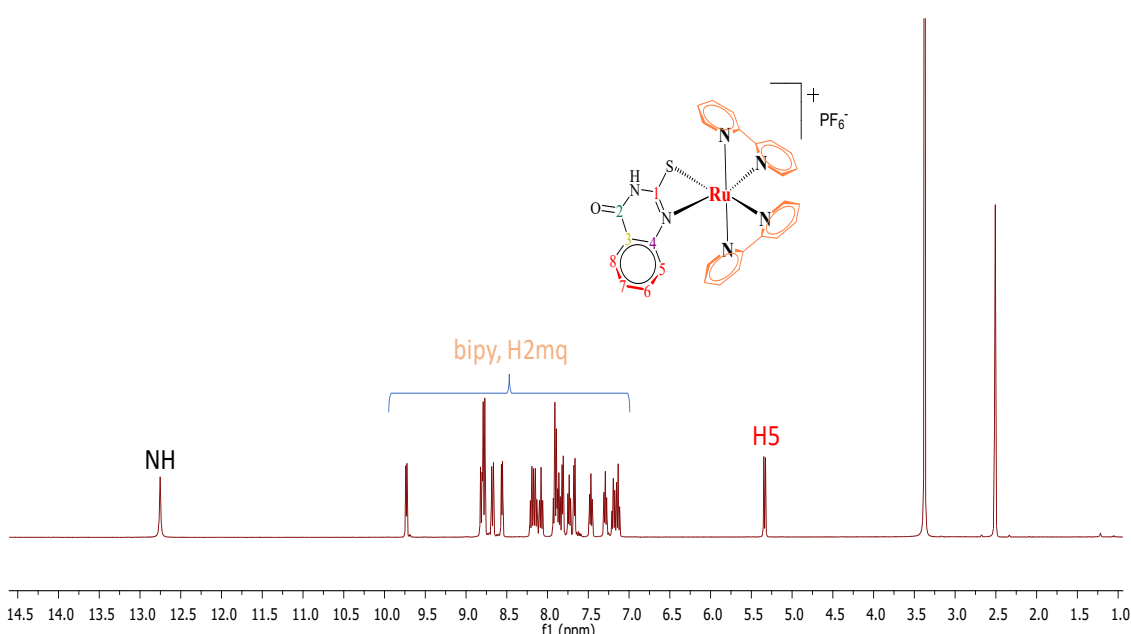


Figure S24. ^1H NMR spectrum of the **Ru5** complex in DMSO- d_6 .

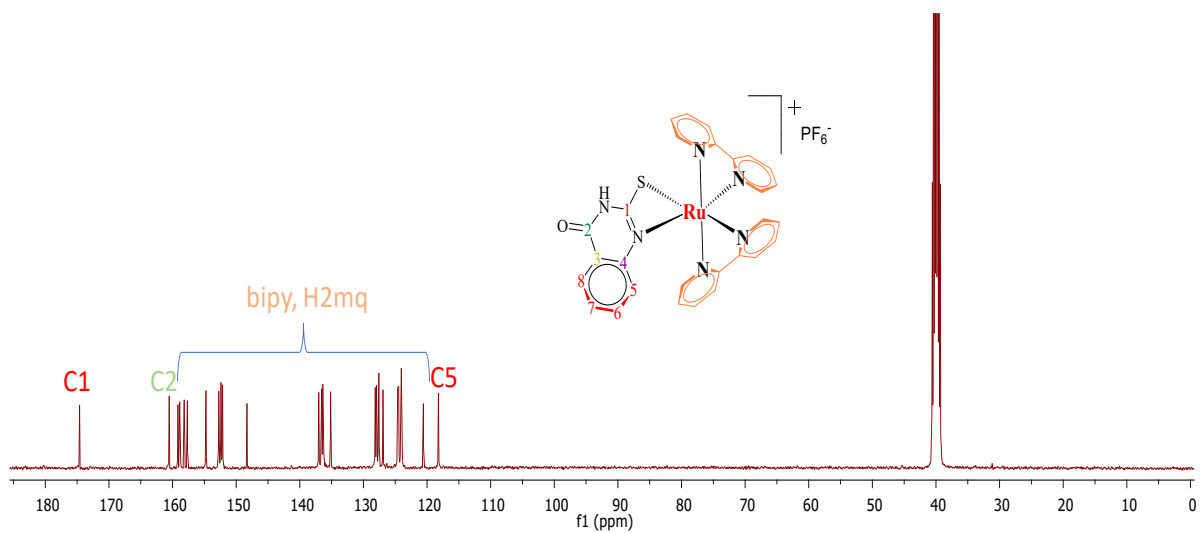


Figure S25. $^{13}\text{C}\{\text{H}\}$ NMR spectrum of the Ru5 complex in DMSO-d₆.

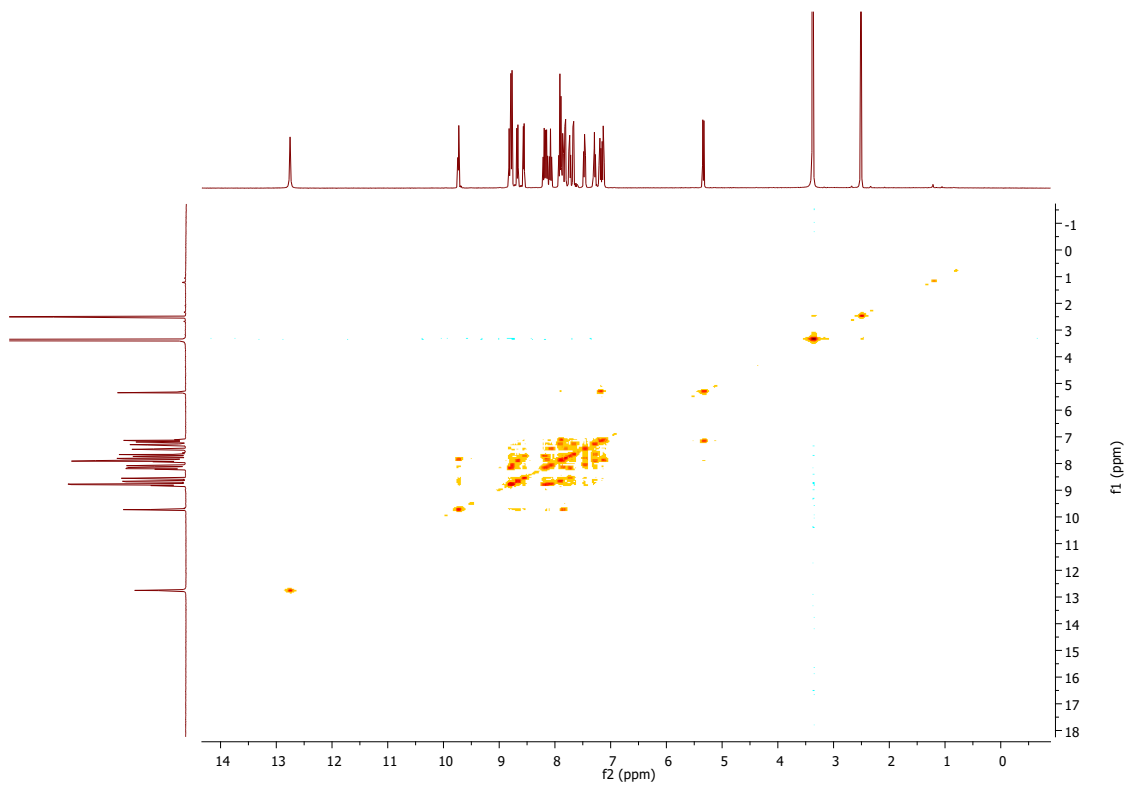


Figure S26. Contour map of the ^1H - ^1H COSY correlation obtained for the Ru5 complex (DMSO-d₆).

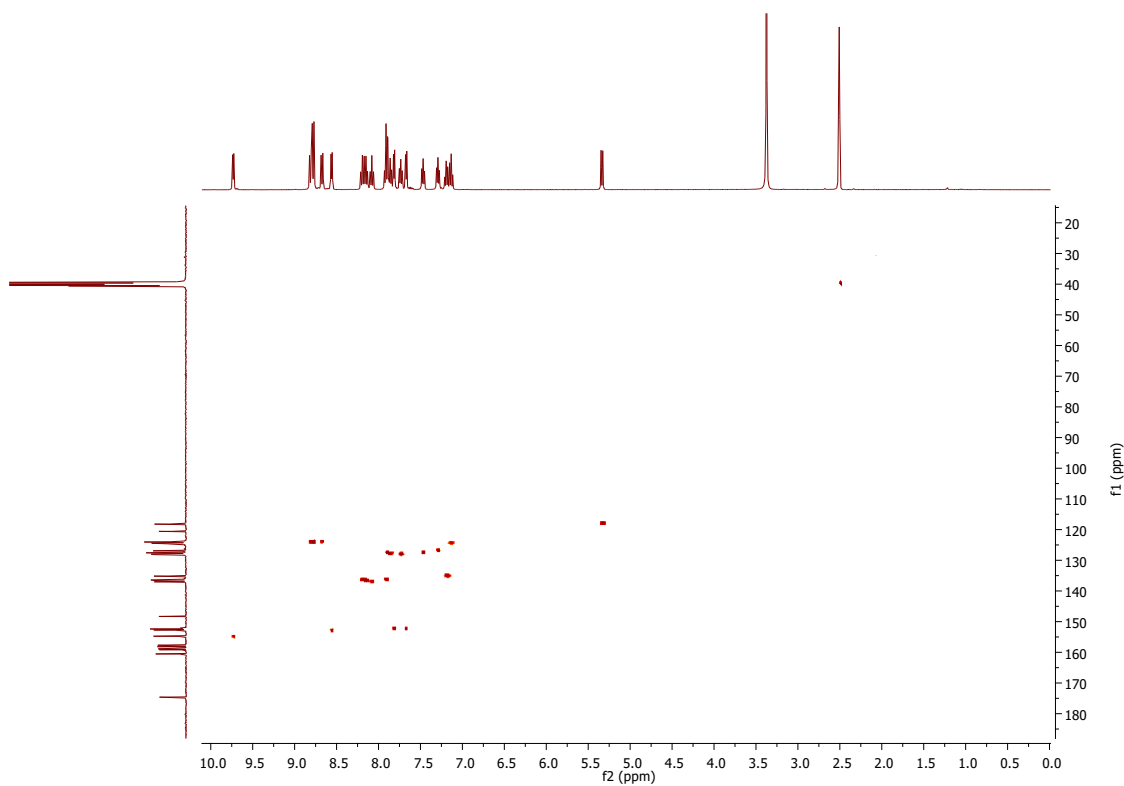


Figure S27. Contour map of the ^1H - ^{13}C HSQC correlation obtained for the **Ru5** complex (DMSO- d_6).

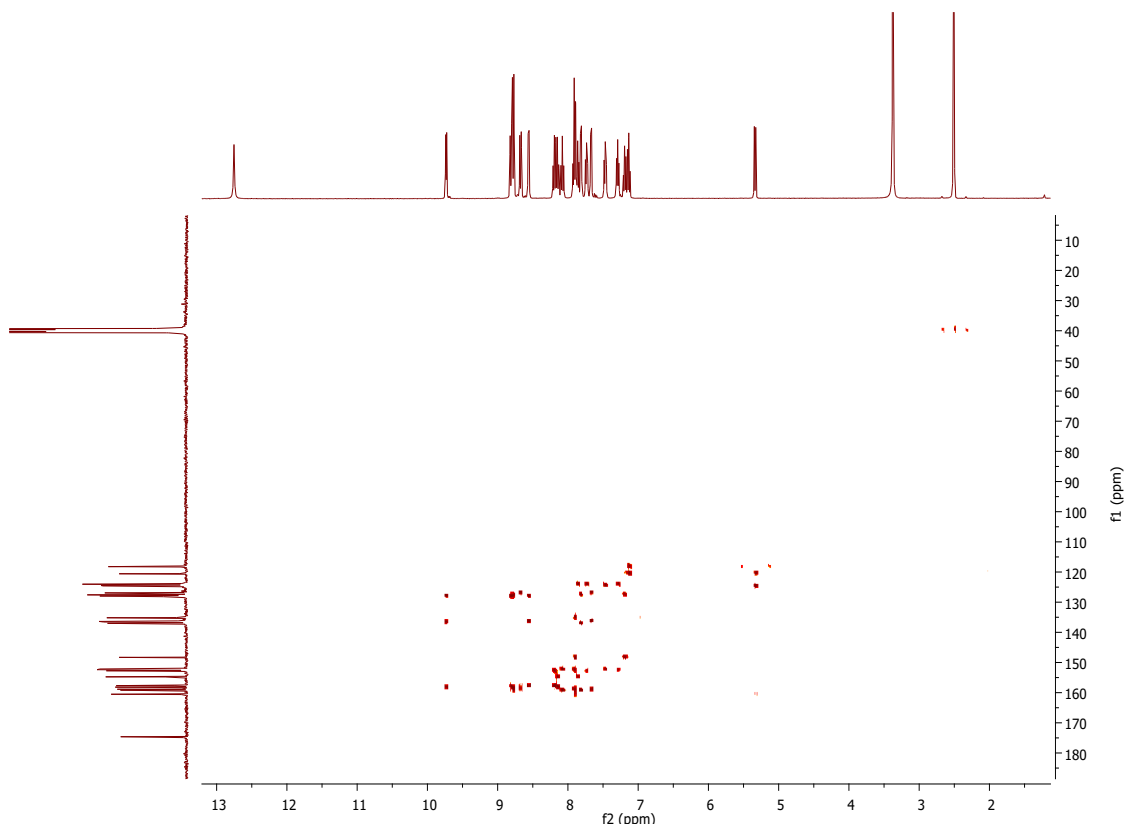


Figure S28. Contour map of the ^1H - ^{13}C HMBC correlation obtained for the **Ru5** complex (DMSO- d_6).

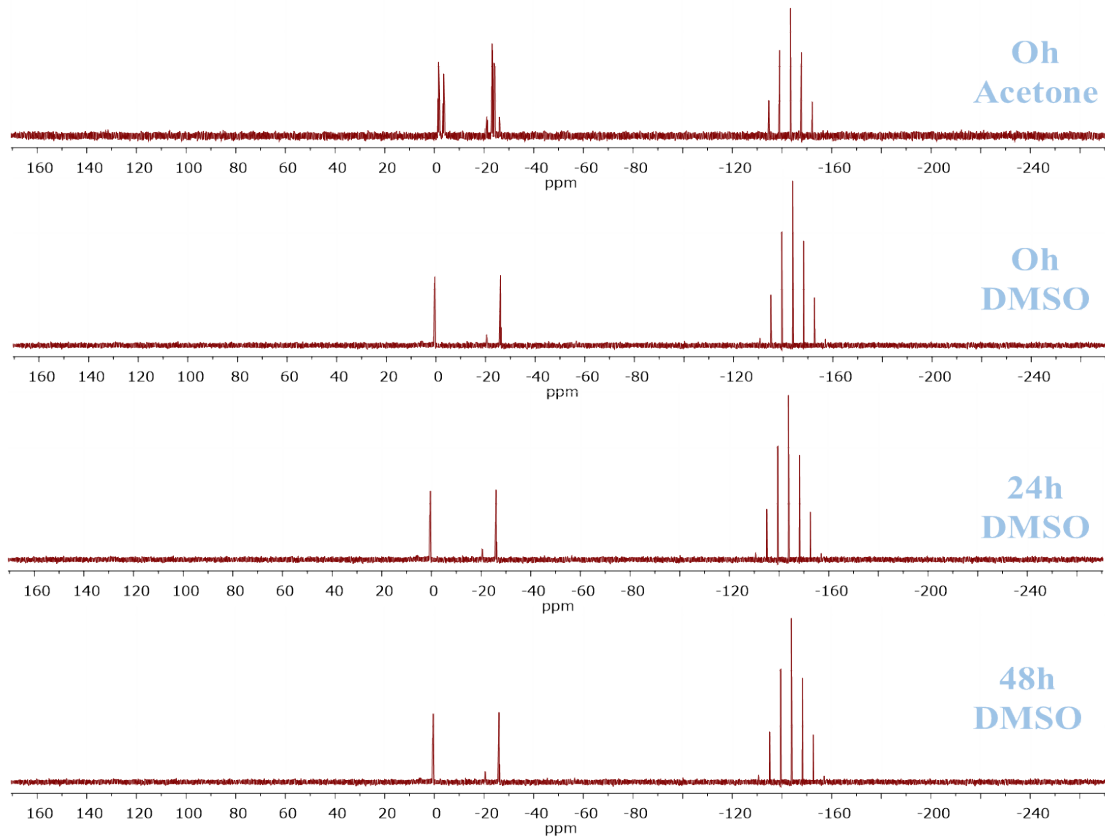


Figure S29. $^{31}\text{P}\{\text{H}\}$ NMR spectra in acetone and DMSO of Ru1 at different times.

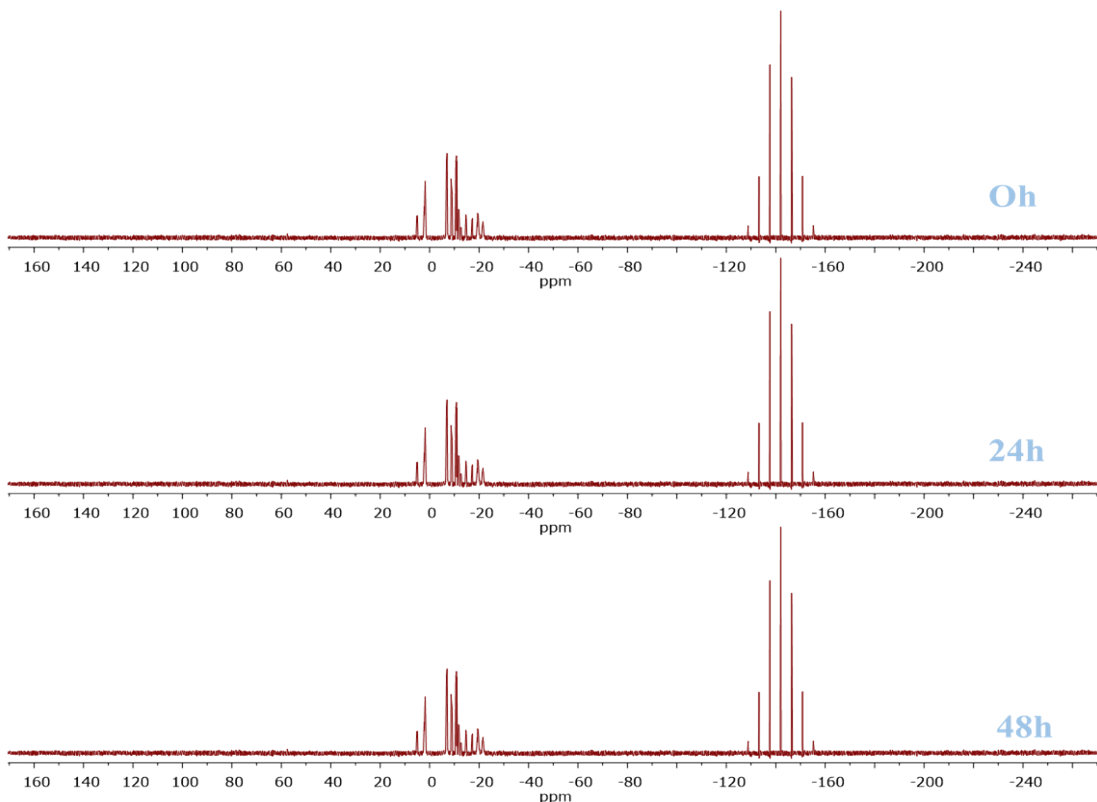


Figure S30. $^{31}\text{P}\{\text{H}\}$ NMR spectra in acetone and DMSO of Ru2 at different times.

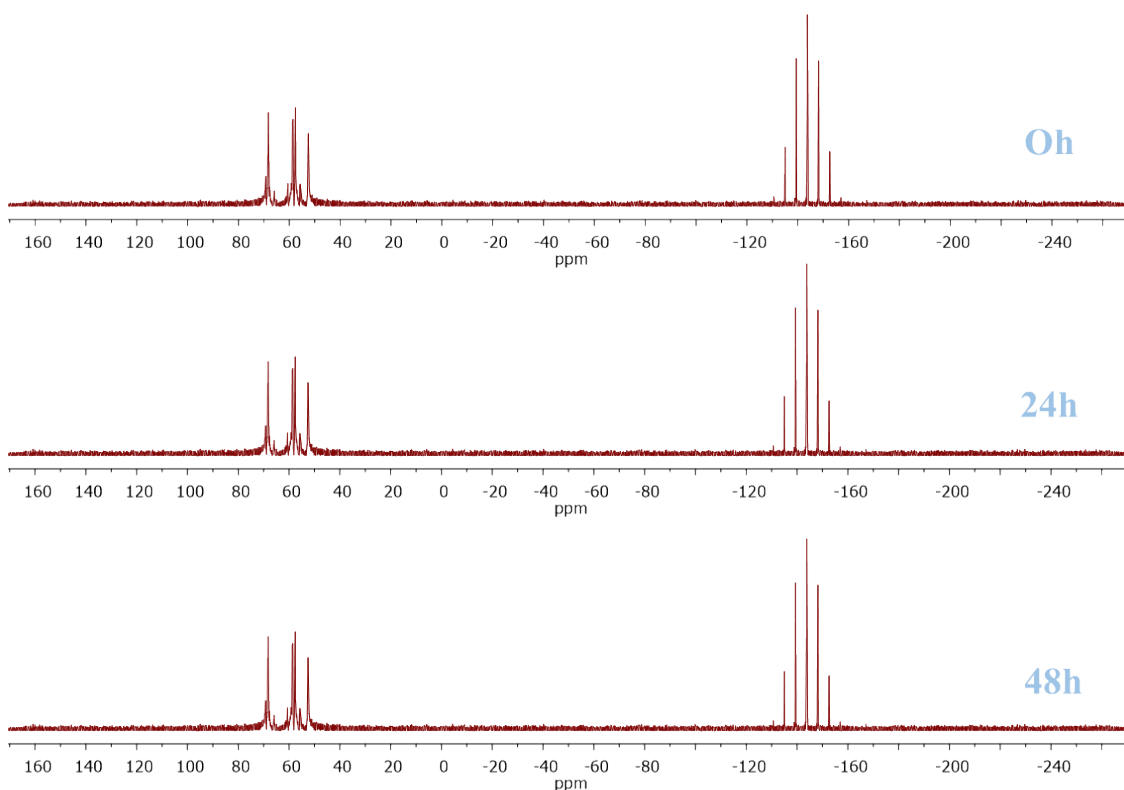


Figure S31. $^{31}\text{P}\{\text{H}\}$ NMR spectra in acetone and DMSO of **Ru4** at different times.

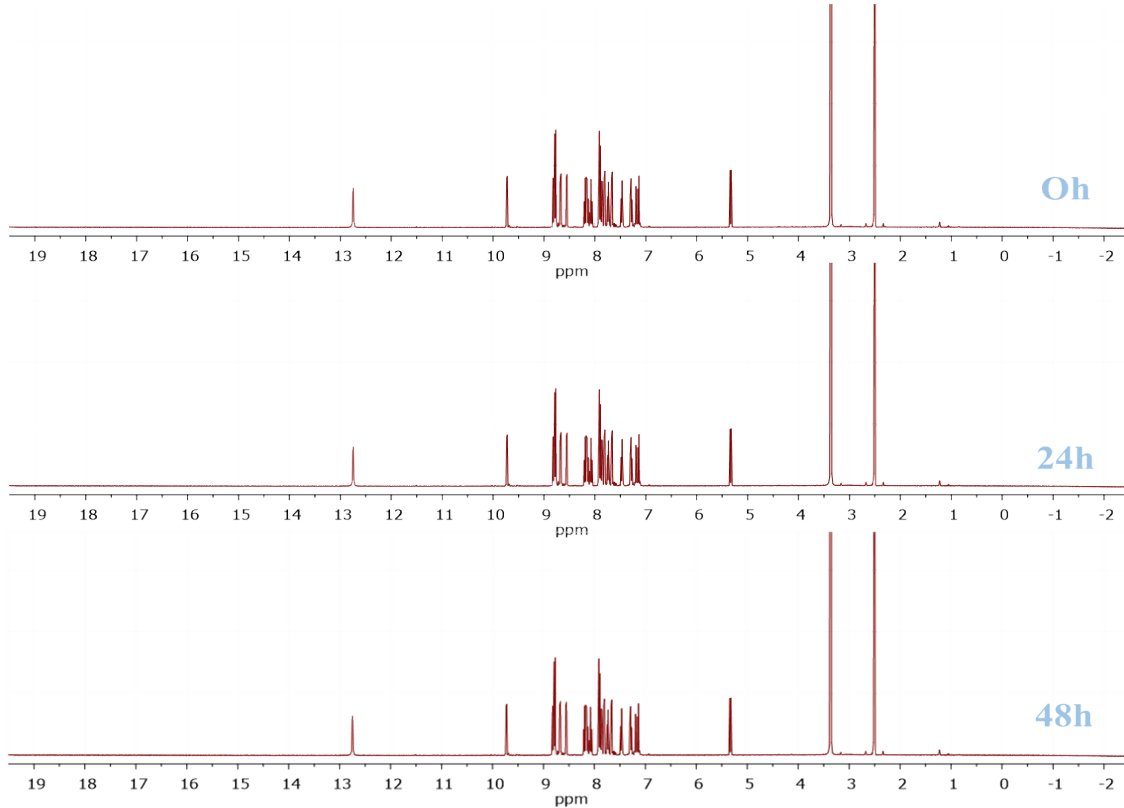


Figure S32. ^1H NMR spectra in acetone and DMSO of **Ru5** at different times.

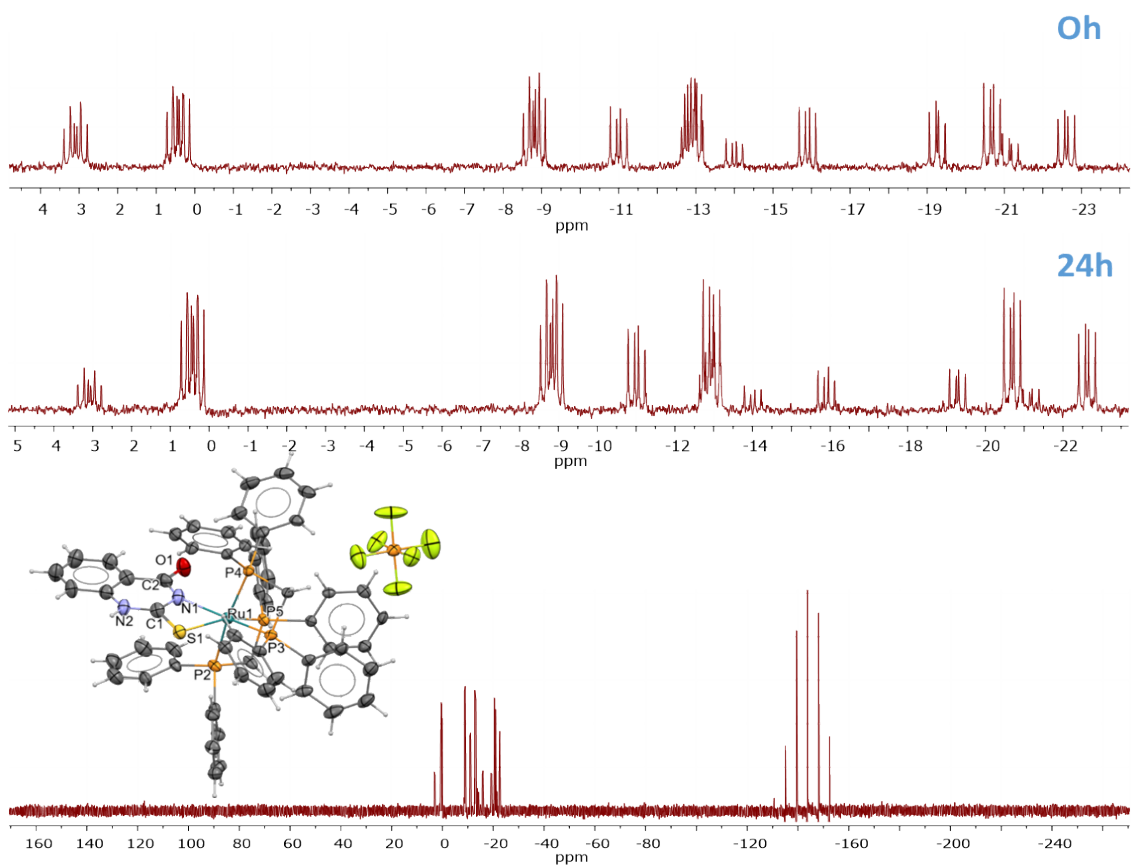


Figure S33. $^{31}\text{P}\{\text{H}\}$ NMR spectra in Acetone/culture medium of **Ru1** at different times and crystal obtained from this solution.

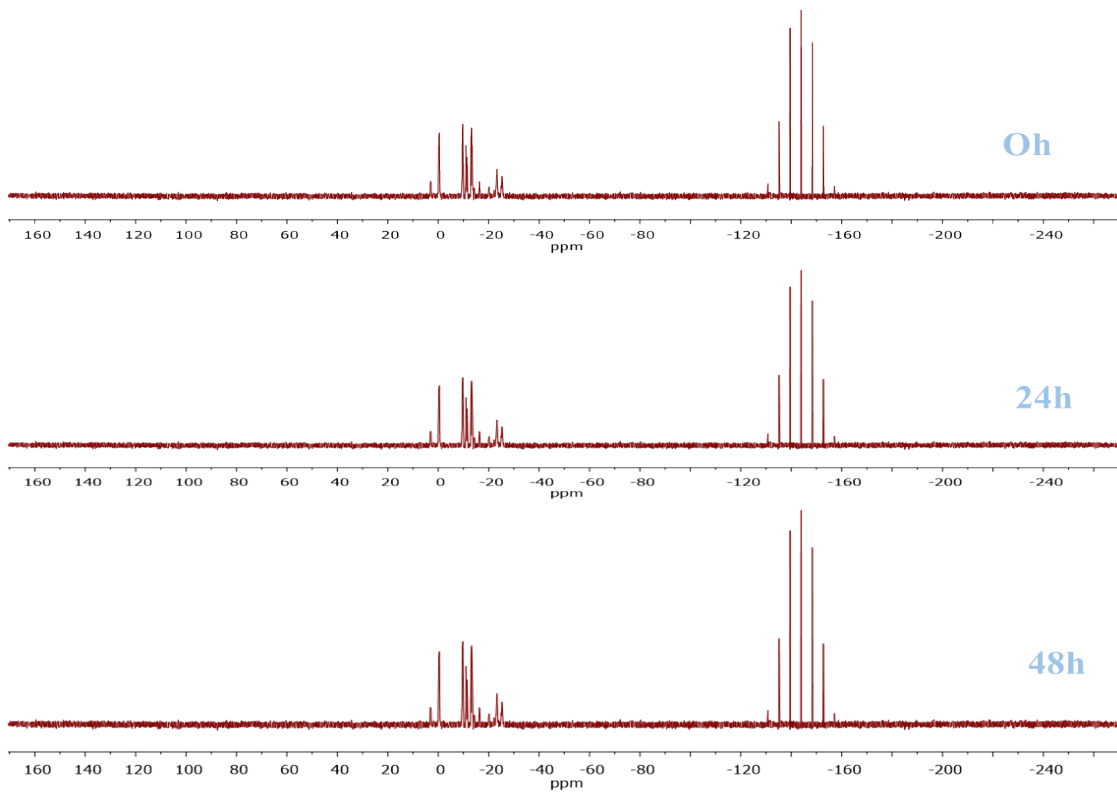


Figure S34. $^{31}\text{P}\{\text{H}\}$ NMR spectra in DMSO/culture medium of **Ru2** at different times.

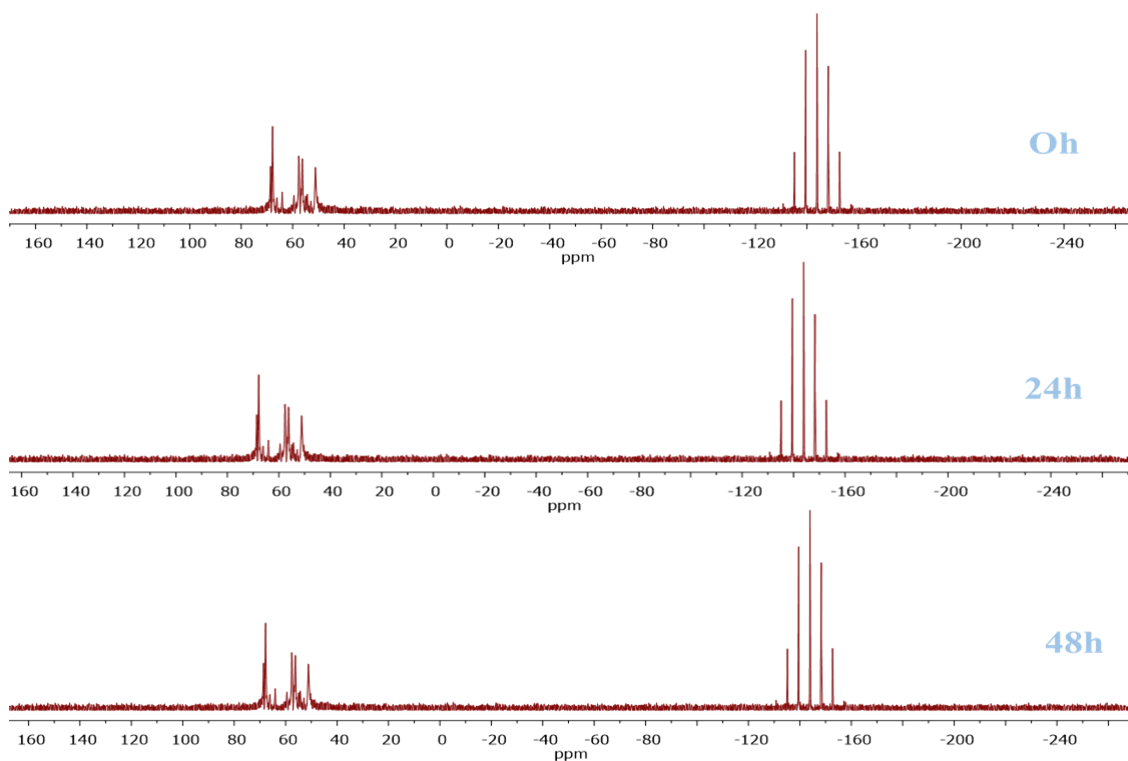


Figure S35. $^{31}\text{P}\{\text{H}\}$ NMR spectra in DMSO/culture medium of **Ru4** at different times.

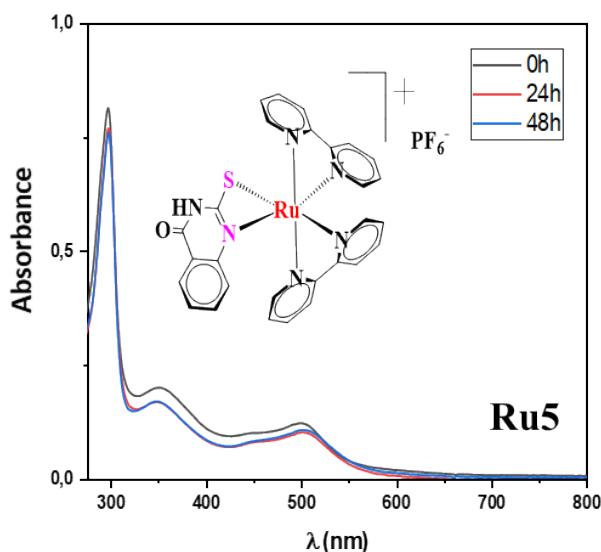


Figure S36. UV-Vis spectra in DMSO/culture medium of **Ru5** at different times.

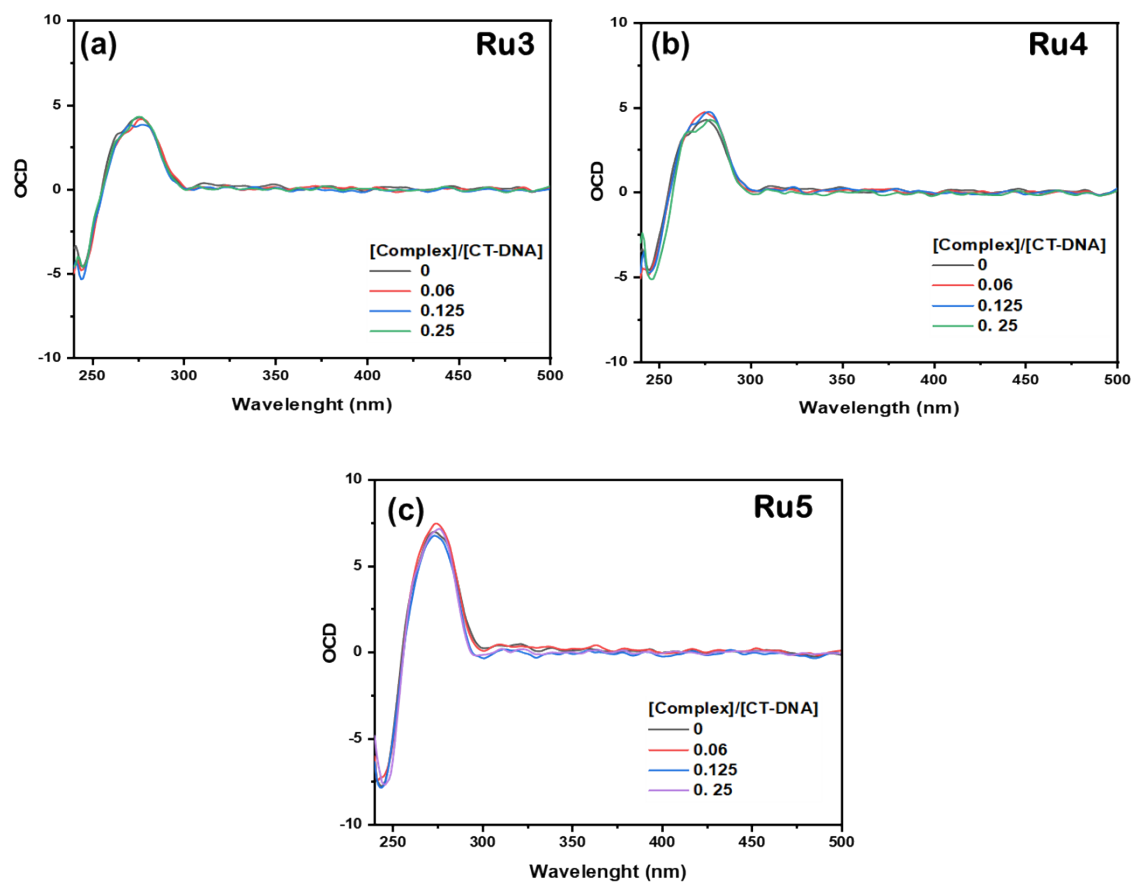


Figure S37. (A-C) Circular dichroism spectra of CT-DNA in absence and presence of **Ru3-Ru5** complexes at different molar ratios (R_i) = [complex]/[CT-DNA] = 0.06 – 0.25.

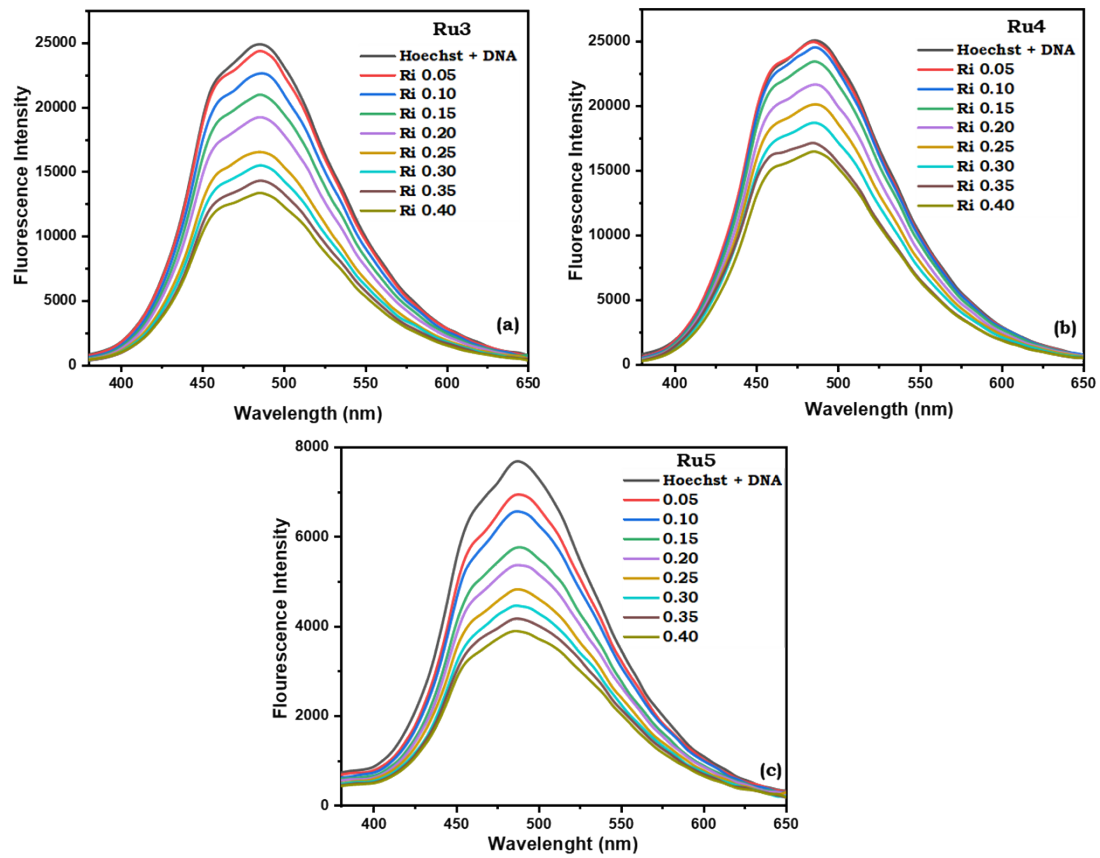


Figure S38. (A-C) Fluorescence quenching of CT-DNA-Hoechst ($\lambda_{\text{ex}} = 343 \text{ nm}$) in the absence and presence of different concentrations of **Ru3-Ru5** complexes.

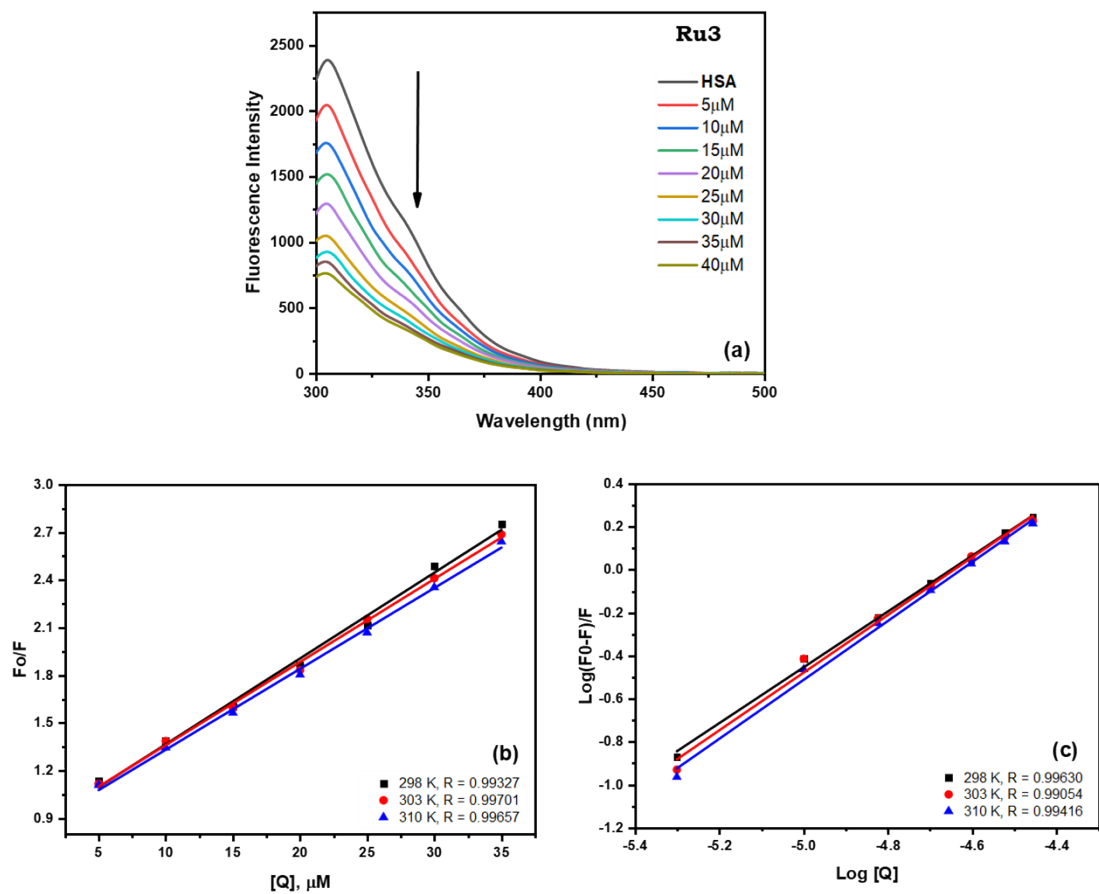


Figure S39. (A) Fluorescence spectra of HSA (5 μM, $\lambda_{\text{ex}} = 270$ nm) in the absence and presence of **Ru3** complex at different concentrations. (B) Stern-Volmer plot and (C) Plot of $\log[(F_0 - F)/F]$ vs. $\log [Q]$, at 298, 303 and 310K.

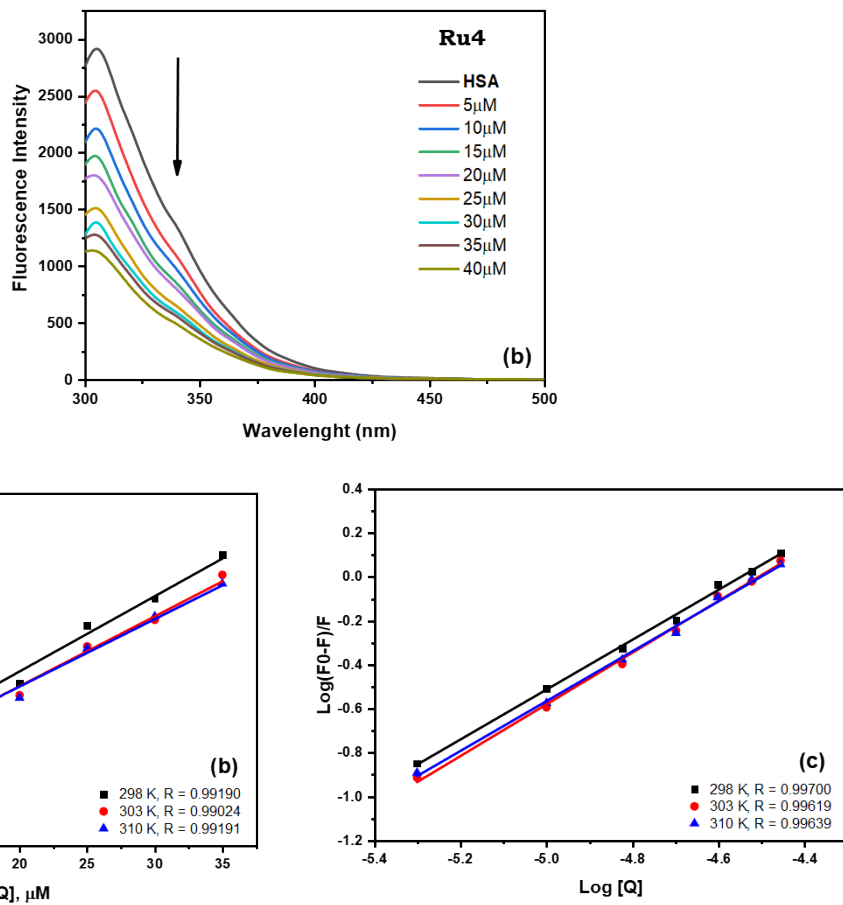


Figure S40. (A) Fluorescence spectra of HSA (5 μ M, $\lambda_{\text{ex}} = 270$ nm) in the absence and presence of **Ru4** complex at different concentrations. (B) Stern-Volmer plot and (C) Plot of $\log[(F_0 - F)/F]$ vs. $\log [Q]$, at 298, 303 and 310K.

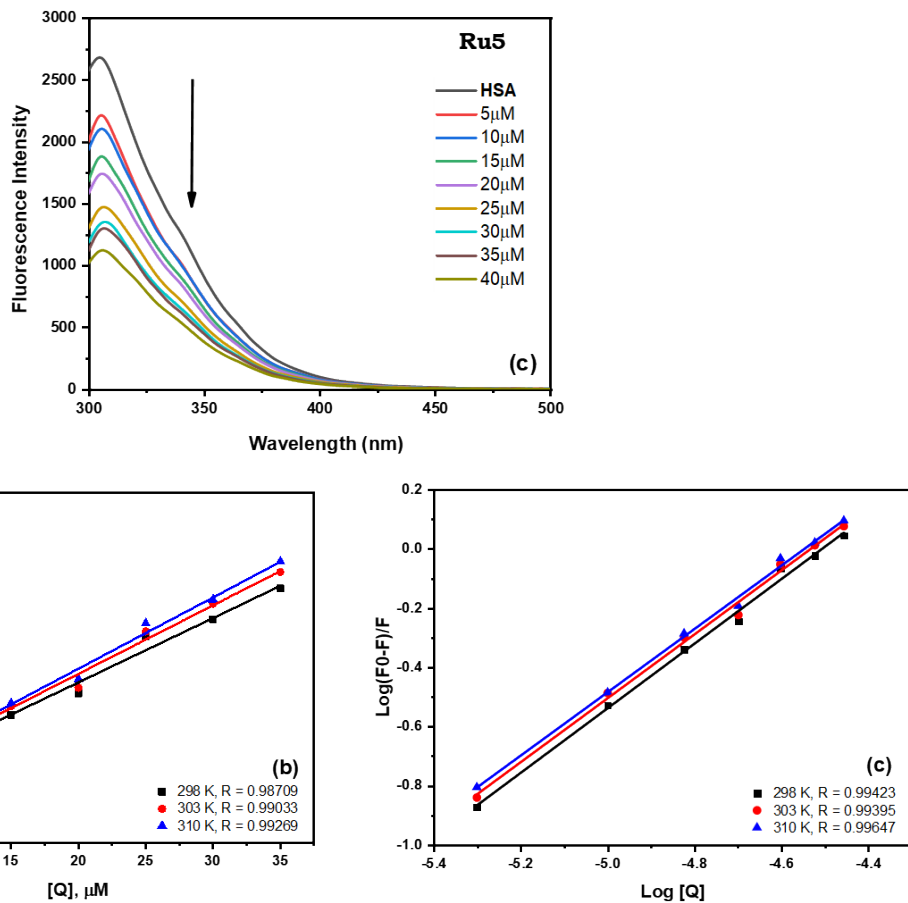


Figure S41. (A) Fluorescence spectra of HSA (5 μM, $\lambda_{ex} = 270$ nm) in the absence and presence of **Ru5** complex at different concentrations. (B) Stern-Volmer plot and (C) Plot of $\log[(F_0 - F)/F]$ vs. $\log [Q]$, at 298, 303 and 310K

Table S1. Values of coupling constant $^2J_{P-P}$ for the **Ru1**, **Ru2**, **Ru3** and **Ru4** complexes

Complex	Phosphorus atoms	δ	$^2J_{P-P}$
Ru1	P1	-2.66	41.7; 28.5
	P2	-4.73	38.2; 27.9
	P3	-23.09	324.0; 41.8; 27.4
	P4	-25.98	323.8; 38.5; 29.3
Ru2	P1	-0.14	43.5; 27.2; 24.0
	P2	-8.02	41.2; 24.9
	P3	-10.87	314.4; 43.5; 26.5
	P4	-21.94	314.5; 41.2; 27.7
Ru3	P1	66.79	23.2
	P2	57.29	291.5; 25.1
	P3	47.97	25.4; 12.4
	P4	42.73	288.6; 22.5; 12.3
Ru4	P1	67.87	m
	P2	59.12	m
	P3	57.15	m
	P4	52.17	m

Table S2. Crystal data and structure refinement parameters obtained for the **Ru1**, **Ru2**, **Ru5** complexes.

Complex	Ru1	Ru2	Ru5
CCDC code	2355448	2355449	2355450
Empirical formula	C ₅₈ H ₅₀ ClF ₆ N ₂ OP ₅ RuS	C ₆₃ H ₆₁ F ₆ N ₂ O ₃ P ₅ RuS	C ₂₈ H ₂₃ F ₆ N ₆ O ₂ PRuS
Formula weight	1275.27	1.296.188	753.629
Temperature/K	100	100	100
Crystal system	monoclinic	monoclinic	monoclinic
Space group	P2/c	Pn	C2/c
a/Å	17.7150(2)	15.2901(3)	21.8405(3)
b/Å	11.48250(12)	11.7639(3)	13.02075(15)
c/Å	28.1918(3)	16.7665(2)	21.5213(3)
α/°	90	90	90
β/°	99.3892(12)	94.0784(16)	108.6637(13)
γ/°	90	90	90
Volume/Å ³	5657.75(12)	3008.18(10)	5798.37(13)
Z	4	2	8
ρ _{calcd} /cm ³	1.497	1.431	1.727
μ/mm ⁻¹	0.57	4.244	6.280
F(000)	2608	1340	3041.1
Crystal size/mm ³	0.128 × 0.119 × 0.05	0.149 × 0.127 × 0.069	0.251 × 0.192 × 0.075
Radiation	Mo Kα (λ = 0.71073)	Cu Kα (λ = 1.54184)	Cu Kα (λ = 1.54184)
2Θ range for data collection/°	3.838 to 51.5	9.2 to 140.14	8.02 to 158.86
Index ranges	-19 ≤ h ≤ 21, -13 ≤ k ≤ 14, -34 ≤ l ≤ 34	-19 ≤ h ≤ 19, -15 ≤ k ≤ 14, -18 ≤ l ≤ 21	-27 ≤ h ≤ 27, -16 ≤ k ≤ 16, -26 ≤ l ≤ 27
Reflections collected	43832	71455	33080
Independent reflections	10730 [R _{int} = 0.0361, R _{sigma} = 0.0234]	9784 [R _{int} = 0.0874, R _{sigma} = 0.0757]	6203 [R _{int} = 0.0537, R _{sigma} = 0.0390]
Data/restraints/parameters	10730/948/811	9784/215/724	6203/0/397
Goodness-of-fit on F ²	1.111	1.044	1.037
Final R indexes [I>=2σ (I)]	R ₁ = 0.0433, wR ₂ = 0.1008	R ₁ = 0.0586, wR ₂ = 0.1445	R ₁ = 0.0359, wR ₂ = 0.0906
Final R indexes [all data]	R ₁ = 0.0484, wR ₂ = 0.1047	R ₁ = 0.0615, wR ₂ = 0.1468	R ₁ = 0.0375, wR ₂ = 0.0916
Largest diff. peak/hole / e Å ⁻³	0.85/-0.59	1.18/-0.41	0.94/-1.22

Table S3. Selected bond lengths (Å) and angles for **Ru1**, **Ru2** and **Ru5** complexes.

	Ru1	Ru2	Ru5
C1-S1	1.727(5)	1.734(7)	1.712(3)
C1-N1	1.337(6)	1.373(9)	1.329(3)
Ru1-P1	2.347(8)	2.368(5)	--
Ru1-P2	2.340(8)	2.320(5)	--
Ru1-P3	2.385(8)	2.358(5)	--
Ru1-P4	2.320(8)	2.301(6)	--
Ru1-N1	--	2.159(14)	2.137(2)
Ru1-S1	2.427(9)	2.439(5)	2.439(6)
Ru1-N3	--	--	2.055(2)
Ru1-N4	--	--	2.048(2)
Ru1-N5	--	--	2.052(2)
Ru1-N6	--	--	2.054(2)
Ru1-Cl1	2.461(8)	--	--
P2 -Ru1-P1	70.73(3)	71.379(18)	--
P3-Ru1-P4	71.84(3)	71.557(18)	--
S1-Ru1-N1	--	66.70(4)	67.21(6)
S1-Ru1-C11	89.83(4)	--	--
S1-C1-N1	123.9(3)	110.38(12)	113.06(19)
N5-Ru1-N6	--	--	78.84(9)
N3-Ru1-N4	--	--	79.07(9)

Table S4. Flow times and confidence limits obtained from the viscosity experiments.

	Ru2	Ru3	Ru4	Ru5	Thiazole	Cisplatin
[uM]						
5	94.50 ± 0.34	84.64 ± 0.19	80.39 ± 0.30	79.33 ± 0.51	72.93 ± 0.28	93.73 ± 0.25
10	95.50 ± 0.29	84.57 ± 0.24	80.47 ± 0.17	78.40 ± 0.22	73.28 ± 0.16	93.24 ± 0.21
20	96.00 ± 0.13	84.60 ± 0.24	81.39 ± 0.30	79.71 ± 0.43	74.03 ± 0.19	90.60 ± 0.20
25	94.89 ± 0.20	84.85 ± 0.27	81.52 ± 0.24	78.93 ± 0.23	74.33 ± 0.23	90.30 ± 0.20
30	95.35 ± 0.15	85.13 ± 0.12	81.38 ± 0.33	78.21 ± 0.20	75.28 ± 0.23	89.28 ± 0.19
40	95.90 ± 0.22	85.73 ± 0.29	81.56 ± 0.32	79.37 ± 0.37	78.23 ± 0.08	87.51 ± 0.37

Table S5. Binding constants (kb) of Ru2-Ru5 with DNA calculated from DNA competition assays using Hoechst 33258.

Complex	Kb
Ru2	2.47 x 10 ⁷ ± 4.69
Ru3	3.13 x 10 ⁷ ± 2.61
Ru4	6.92 x 10 ⁶ ± 2.11
Ru5	5.44 x 10 ⁴ ± 1.05

Table S6. The thermodynamic interaction parameters of the Ru2-Ru5 complexes with HSA.

Complex	N	ΔH° (kJ mol ⁻¹)	ΔS° (J mol ⁻¹ K)	ΔG° (kJ mol ⁻¹)
Ru2	0.90	-2.9	115.3	-25.7
	0.89		115.3	-26.3
	0.86		115.0	-27.0
Ru3	0.79	-4.4	115.0	-26.3
	0.76		115.0	-27.0
	0.73		74.8	-27.5
Ru4	0.92	-12.4	80.1	-26.8
	0.91		80.1	-27.2
	0.85		79.7	-27.6
Ru5	0.80	8.7	45.9	-26.0
	0.86		45.9	-26.3
	0.89		45.5	-26.8